TÉCNICO LISBOA

Removal of Added Value Alkaloids from Food Aqueous Streams

Master Thesis Dissertation

Ana Filipa Nascimento Quintino

Master in Biotechnology

Advisor(s)/Supervisor(s): Prof.Dr. Frederico Castelo Ferreira
Prof.Dr. Teresa Sofia Araújo Esteves

Examination Committee

Chairperson: Prof.Dr. Marília Clemente Velez Mateus
Supervisor: Prof.Dr.Teresa Sofia Araújo Esteves
Members of the Committee: Prof.Dr. Flávio Alves Ferreira

December 2021

Preface

The work presented in this thesis was performed at the Institute for Bioengineering and Biosciences of Instituto superior Técnico (Lisbon, Portugal), during the period September2020-August2021, under the supervision of Prof. Frederico Ferreira and Prof. Teresa Esteves.

Abstract

This thesis focuses on two food products, lupin beans and bitter oranges, that could help release some of the pressure on agriculture and natural resources.

These food products, have good nutritional value and as crops, have low water consumption and are very resistant to temperature changes and soil acidity. The main issue with these are the toxic compounds that make them not edible (synephrine in bitter orange and Lupanine in Lupin beans). This toxicity causes bitter oranges to be wasted and the need to spend large amounts on the industrial food processing of lupin beans to make its consumption safe.

The mentioned toxic compounds are added value compounds that the pharmaceutical industry uses. The present work considers the use of adsorptive separation methods to remove and recover these toxic compounds with pharmaceutical properties, allowing the safe consumption of the food while seeking to decrease its environmental impact.

Lupanine binding percentage for commercial polybenzimidazole (PBI) polymer and three derived PBIs were studied for different solutions, the treated PBIs showed improved results compared to the commercial PBI. Optimizations, adsorption isotherms and binding kinetics were also studied, and several recovery solvents were tested to recover lupanine after the binding.

Bitter Oranges amines were extracted with water and the flavonoids were extracted with ethanol a preliminary binding assay was performed with a synthetic mixture of bitter orange juice (from which the acidic resins were the best to bind synephrine) the extracted compounds were analysed and quantified (493 ppm of synephrine).

Keywords: Food production, lupin beans debittering effluent, lupanine, bitter orange, synephrine, polybenzimidazole polymer (PBI))

Resumo

Esta tese concentra-se em dois produtos alimentares, o tremoço e a laranja amarga, que podem aliviar parte da pressão sobre a agricultura e os recursos naturais.

Esses produtos alimentares, possuem bons valores nutricionais e na agricultura tem baixos consumos de água, são resistentes às mudanças de temperatura e à acidez do solo. O problema destes alimentos são os compostos tóxicos que impedem o seu consumo (sinefrina na laranja amarga e lupanina no tremoço). Essa toxidade faz com que as laranjas amargas sejam desperdiçadas e se tenha de gastar muita água no processamento industrial dos tremoços para tornar seu consumo seguro.

Os compostos tóxicos mencionados são compostos de valor acrescentado usados pela indústria farmacêutica. O presente trabalho propõe a utilização de métodos de separação por adsorção para remoção e recuperação desses compostos tóxicos com propriedades farmacêuticas, permitindo o seu consumo seguro e tentando diminuir seu impacto ambiental.

A percentagem de adsorção da lupanina para o polímero polibenzimidazol (PBI) comercial e três PBIs derivados foram estudados para diferentes soluções, os PBIs derivados foram melhores em comparação com o PBI comercial. Otimizações, isotermas de adsorção e cinética de adsorção foram estudadas. Testou-se vários solventes de recuperação para recuperar a lupanina após a adsorção.

As aminas da laranja amarga foram extraídas com água e os flavonóides foram extraídos com etanol. Um ensaio de ligação preliminar foi realizado com uma mistura sintética de sumo de laranja amarga (resinas ácidas ligaram melhor a sinefrina), os compostos extraídos foram analisados e quantificados (493 ppm de sinefrina).

Keywords: Produção de alimentos, efluente do adoçamento do tremoço, lupanina, laranja amarga, sinefrina, polibenzimidazol (PBI)

Agradecimentos

Quero agradecer em primeiro lugar aos meus orientadores, aos professores Frederico Ferreira e Teresa Esteves, que mesmo durante a pandemia e com filhos pequenos em casa sempre arranjaram tempo e disponibilidade para me acompanhar e orientar (mesmo que por poucas vezes só por zoom e à hora da sesta), obrigado por me terem deixado fazer parte deste projecto e por confiarem em mim para continuar o meu trabalho no laboratório mesmo durante o confinamento geral, esta tese não teria sido possível sem o vosso apoio muito obrigada.

Obrigada também a todas as pessoas que no laboratório que me ajudaram desde o primeiro dia que cheguei: ao Ricardo pela sua paciência para procurar equipamentos e materiais; à Dona Rosa, por ter sempre pontas das pipetas guardadas para o nosso laboratório e por ter sempre uma palavra amiga e estar sempre disponível para me ajudar apesar de estar sempre cheia de trabalho; ao Helvio e a Leonor e aos outros MSc como a Maria, a Matilde, a Inês, a Filipa e o Alexandre que mesmo com distanciamento físico e mascaras na cara estavam sempre com um sorriso amigo, e não me posso esquecer do Flávio que das poucas vezes que esteve comigo teve sempre uma alegria contagiante boa disposição sendo das primeiras pessoas que conheci no laboratório.

Quero também agradecer à minha família, que sempre me apoiou em todas as etapas da minha vida incluindo esta: ao meu pai, pelo microscópio, as idas aos museus, os documentários ao domingo de manhã, etc. tudo isso fez com que eu acabasse por escolher o caminho que me levou a acabar este mestrado; obrigada também a minha mãe, que foi a minha ajuda durante todo este tempo, obrigada por cuidares de mim, garantires que tinha roupa lavada e comida para levar para a universidade, muito obrigada por imprimires todos os meus documentos e vires carregada com eles até casa, por me ouvires desabafar, seres a minha confidente e por me motivares a ser melhor e a nunca desistir e claro aos meus dois pais obrigado por me terem pago as propinas; Obrigda também ao meu irmão mais novo o Tiago, a minha avó Tina, a minha avó céu e também ao meu avô Zé que infelizmente já não me viu acabar o curso, muito obrigada por todo o vosso apoio. Obrigada também ao Bruno, por te preocupares comigo me ouvires e apoiares durante este ultimo ano, por todo o carinho e por me ires buscar à universidade de vez em quando. Às minhas amigas, à Sara e à Marlene, obrigada por serem minhas amigas do coração e não importar quanto tempo passe sempre que preciso estão cá para mim obrigada também à Susana, à Narmin, à Mariana, à Raquel à Sofia, ao Filipe e a todos que me apoiaram durante estes ultimos meses.

Contents

List of Tables

List of Figures

Acronyms

AcOH glacial acetic acid.

BSA Bovine Serum Albumin.

CA Citrus aurantium L.

DCM dichloromethane.

DMSO Dimethyl sulfoxide.

DNS 3,5-dinitrosalicylic acid.

EtOAc Ethyl acetate.

FDA Food and Drug Administration.

GAE Gallic Acid Equivalent.

GGE Greenhouse Gas Emissions.

HCl hydrochloric acid.

HPLC High Performance Liquid Chromatography.

IPA isopropanol.

IPCC Intergovernmental Panel on Climate Change.

KOH potassium hydroxide.

MeCN acetonitrile.

MeOH methanol.

NaOH sodium hydroxide.

PBI polybenzimidazole.

THF tetrahydrofuran.

Chapter 1

Motivation and Objectives

Society is starting to feel today the effects of climate change. The rising temperatures, extreme weather, lack of potable water and biodiversity loss are some of the many problems that will continue to affect human life and food production in the following years, harsh environments make it harder to produce food.

Even though climate change will affect the food industry, it is itself responsible for causing it. For example, over 70% of all freshwater withdrawals from rivers, lakes, and aquifers are necessary to irrigate agricultural fields[1,2]; also, animal production causes up to 18% of the total human-induced greenhouse emissions[3]. To reduce these numbers, we cannot affect production as it is crucial for human life, so we need to keep producing food while reducing its environmental impact.

This work focuses on exploring the sustainability potentials of two food products, Lupin Beans and Bitter Oranges. We selected these because they require scant amounts of water to grow [4, 5], as they don't need irrigation. They are also resilient to high temperatures and changes in soil pH [6, 7], growing even under climate change challenging conditions. Also, lupin beans are natural fertilisers [8], natural pesticides [9], and have a high protein content being an alternative to meat and could reduce the need for animal protein consumption [10, 11]. The fundamental problem with these products in the food industry is the natural toxic alkaloids which extraction is required before consumption [12]. So, the food industry does not use bitter orange fruits today, mainly the peals are used to produce food additives and flavours, the rest is lost [13, 14]. Even though its fruits are full of healthy antioxidant flavonoids, it's alkaloid (synephrine) prevents it's consumption [15]. On the other hand, the food industry already widely uses lupin beans, but removing their main alkaloid (lupanine) implies the use of huge amounts of water [16], so this process needs to be optimized to extract lupanine while reducing water consumption.

These toxic compounds, that need to be removed from the fruits and seeds, are added value compounds. They are starting materials used by the pharmaceutical industries. By isolating only synephrine, from the bitter orange juice, it can be sold to the pharmaceutical industry and keep the antioxidant properties of the juice unchanged. Another approach would be to also isolate these healthy flavonoids and used them as additives to produce new antioxidant and possibly antiviral and anti-inflammatory food products.

So, our main goal is to decrease waste and water consumption while removing the toxic added value compounds to make lupin beans and bitter orange sustainable and healthy food products.

To achieve the aim of this thesis, several points were well-defined:

- Lupin beans:

    1. The industrial lupin bean effluent, where the lupanine is present, was characterised.

2. Different polybenzimidazole (PBI) derived adsorbers were obtained and tested for lupanine binding.
3. Different solvents were evaluated for lupanine recovery from the adsorber after binding with the different PBI adsorbers.

- Bitter Orange:

1. Bitter orange fruits were dried and the alkaloids and flavonoids were extracted with water and ethanol respectively.
2. An HPLC method was developed for identification and quantification of the different compounds present in bitter orange extracts.
3. Preliminary assessment of the most suitable commercial resin was performed for synephrine or flavonoid binding and future recovery. To achieve this, a synthetic aqueous mixture of synephrine and naringin (at approximately the pH of the bitter orange juice) was added to different commercial resins.

Chapter 2

Introduction

2.1 Environment and Food Production

According to the United Nations Department of Economic and Social Affairs it is estimated that by 2050 we will be 9.7 billion people (Figure A.1) [17], all of them consuming resources and producing vast quantities of waste, such as pollutants and toxic materials [18, 19].

Sustainably meeting the food demand of a growing population using finite resources while protecting the environment is possibly one of the significant challenges of humanity in the coming decades.

According to the Intergovernmental Panel on Climate Change (IPCC) (2021) [20], global warming is likely to reach a 1.5 ºC increase between 2030 and 2052. At the current rate, climate-related risks to health, livelihoods, food security, water supply, human security, and economic growth are projected to increase with global warming. Also, the effects of this change may be long-lasting or irreversible, such as losing some ecosystems [20].

Since 1970, human activities have wiped out 60$\%$ of wildlife populations [21].The loss of biodiversity is connected to climate breakdown, affecting each other and producing equally serious risks [22]. Not only biodiversity is being lost above ground, but also below ground in the soil. Each year 75 billion tonnes of soil are stripped from the land by wind and water erosion, most of it from agricultural fields [23]. Soil composition regulates the functioning of the ecosystem, and this biodiversity loss threatens ecosystem multifunctionality and sustainability [24]. Global environmental changes and land-use intensification are the strongest drivers of soil biodiversity loss [24–26]. Topsoil is eroding 13 to 40 times faster than nature can replenish it, and if current rates of land degradation continue, most of the topsoil and current agricultural croplands could be gone or severely eroded within 60 years [27].

When this damage to soil is irreparable, it results in desertification, especially in soils with low levels of organic matter because of human activities [24–26] and climatic conditions [23], influenced by global warming [28]. These crises of drought and desertification of soils will affect the crops and animal health, lowering breeding rates [3].

This problem extends beyond the land affecting the sea. The biodiversity of marine ecosystems is in danger because of human activities [29]. Besides that, we are killing trillions of wild aquatic animals every year for food [30]. If we keep fishing at the current pace, by 2048, our oceans will be empty of fish [31].

From these sources, we can understand that our principal sources of protein (meat [3] and fish [31]) are in danger of not being sufficient to keep feeding our increasing population [20].

It is estimated that the frequency and magnitude of extreme climatic events such as storms, floods and droughts will continue to increase because of climate change [20], leading to more soil degradation

and more biodiversity loss that will have severe consequences for agricultural productivity [28]. Losing agriculture productivity and rising demand for food worldwide will intensify the need for industrial agriculture, including more irrigation, the use of fertilisers, biocides and mechanisation, and could also mean a need to expand the croplands and pastures, replacing natural ecosystems [32], all to overcome the losses caused by climate change and overpopulation [22].

Our sources of freshwater are also running dry. About 70% of all freshwater withdrawals from rivers, lakes, and aquifers are used to irrigate agriculture [1,2] and, from these, 70 % are being used for animal production and animal feed [33]. In the future, we may not sustain such an amount with the reservoirs of water rapidly decreasing [2]. It is estimated that over two-thirds of the world's population will be affected by water scarcity over the next decades [34].

Meat production is increasingly less sustainable, requiring high volumes of water per unit of product and the billion land animals contribute to total human-induced greenhouse gas by 18% and total CO_2 emission by 9% [3]. Animal agriculture is estimated to produce more Greenhouse Gas Emissions (GGE) than all forms of transportation combined [35]. Because agriculture production, and consequently food security, is strongly influenced by the changes in environmental conditions [28], it is necessary to respond to the need to produce enough food, feed and fibre sustainably, while satisfying the needs for a non-stopping growing population in a changing climate.

There is a serious risk of future conflicts over habitable lands and natural resources, and forced human migration is expected to rise mainly because climate change effects will affect agriculture in various ways, and it will increase the risk of food security especially for the world most vulnerable people [22]. Currently, in developing countries, there are already millions of people suffering from starvation and malnutrition. Even though we are farming the planet more than ever and producing enough food to feed everyone [36], most of this food goes to waste. Worldwide, tons of good edible food is wasted every day, being estimated that one-third of the food produced is wasted [37]. Although almost a billion people are chronically hungry worldwide [38, 39], millions of people in developed countries are eating more than necessary and suffering from diet-related diseases [40–43].

In conclusion, we have an overpopulation that wastes one-third of all the food produced while millions of people suffer from hunger and malnutrition and millions are obese or overeat. Our food system is too rich in fat, sugar, salt and meat [40], causing health and environmental problems like heart disease and GGE, putting our natural resources under pressure. The sources of freshwater are running out or becoming polluted, the soils are being degraded and the biodiversity of the ecosystems is threatened, with all these effects being increased by climate change. Therefore, our food system needs to be adjusted to provide healthier food to our growing population while reducing waste and environmental impact.

With so many problems to solve, there is no single perfect solution to fix all of them. We need to reduce water usage in agriculture, find alternative sources for animal protein to decrease animal production, reduce the use of fertilisers and pesticides that pollute water sources. This thesis will focus on two food products that meet some of these features and, if optimised, their processing could help diminish some of these problems.

2.1.1 Potential sustainable food products and their main issues.

Lupin beans and bitter orange have good nutritional properties. Lupin beans are a wonderful source of proteins and fibres [10, 11] making them suitable as a meat substitute. Both products' agriculture productions require scant amounts of water to grow [4]. Moreover, they are resistant to a high range of changes in soil pH [44] and temperatures [7]. Lupin beans also work as a natural fertiliser and pesticide and could reduce the number of pollutants used in agricultural fields [8]. The main problem with lupin

beans is that they have in their composition alkaloids, mainly lupanine, that give a bitter taste to the beans and are toxic [45]. Therefore, before consumption, it is necessary to remove them. In this process, a massive amount of water is used in a debittering process, producing lots of waste, throwing away the sustainable benefits of agricultural production [12].

Bitter oranges, although having great potential as sustainable food, are not used by the food industry. Mainly the peals are used to produce food additives, flavours and marmalade, but everything else is wasted [13,14]. The main reason for this is that the rest of the orange is full of toxic alkaloids (synephrine) that make the fruits not edible [46].

One way to correct the environmental issues with these products is to remove the toxic alkaloids from the food matrixes without impairing food quality and decreasing waste generation and water consumption.

Also, these toxic chemicals present in the bitter oranges and lupin beans are added value compounds mainly used by the pharmaceutical industry to make medicines [15, 47, 48]. So, besides having a good adsorption method that binds selectively these alkaloids, we should also have a satisfactory recovery method to further valorise them. This thesis aims to study ways to separate the toxic added-value compounds from the food products while producing sustainable healthy food, decreasing waste and freshwater consumption.

2.2 Lupin Beans

Lupin beans, *Lupinus albus* L. (white lupins), belong to the Leguminosae family, are endemic in the Iberian Peninsula, in the Mediterranean region and have been cultivated for food for over three thousand years, since ancient Greece [49].

2.2.1 Crop properties

White lupin grows well in different climates, from northern Europe and Russia to the arid Australian plains, to the Andean highlands. It is cold-tolerant, but temperatures of -6 ºC to -8 ºC harms germination [7].

Lupinus albus L. is used in agriculture as a natural fertiliser, increasing the amount of organic matter in the soil because of its ability to fix atmospheric nitrogen in the roots through endosymbiosis with bacteria from the Rhizobiaceae family. After harvest, the roots can be collected and sold as a natural fertiliser, decreasing the excessive use of synthetic fertilisers [8]. Because of this ability, it can also grow in infertile soils [50].

It requires meagre amounts of water to grow, *Lupinus albus* L. has intrinsic drought tolerance involving either dehydration avoidance by the maintenance of water uptake or reduction in water loss, or dehydration tolerance by osmotic adjustment [4]. However, a study [51] showed that during this water stress, Lupinus loses most of its leaves and also the stem functioned as a storage repository of sugars (glucose and sucrose) and amino acids (asparagine and proline), but also concluded that upon re-watering, lupin plants rapidly re-established the relative water content.

Lupinus albus L. prefers disturbed sites, poor soils, and areas with reduced competition. It grows well in acidic soils, being more resistant to soil acidity than other legumes such as alfalfa and soybean [44], although its growth is hampered on alkaline soils [7].These characteristics are relevant for the future because of the soil degradation and water scarcity predicted for the next decades [52].

2.2.2 Composition

The composition of Lupinus albus L. is within the following ranges [10, 11]:

- 36-52% protein;
- 5-20% oil;
- 30-40% fibre;
- 2.4 - 6% sugar;
- 1.9- 2.69% alkaloids (with lupanine being the most abundant, close to 70% [11])

Lupin beans also have vitamins and essential amino acids like lysine, leucine and threonine.

Saccharides

The most abundant sugar present in Lupinus albus L. is sucrose representing about 70.7% but also galactose [12], glucose, ribose, maltose, fructose and xylose (Table 2.1). Lupin seeds contain a higher amount of sugar than wheat and legumes, except for soybean [53].

Lupinus usually contain a high percentage of protein and fibre and is therefore used as human food mainly as a snack and in animal feed, being widely used in protein supplements for ruminants [54]. In the food industry, due to its high percentage of protein and high nutritional value, it can be used as a

meat substitute, being used in the manufacture of food products such as flour, crackers, pasta and drinks [55]. But in order to consume the lupin beans, it is necessary to extract the alkaloids, as they are toxic, and they are responsible for the bitter taste.

Table 2.1: Monosaccharide and disaccharide composition of lupin beans (L. albus) [10].

Sugars	Total (%)
Sucrose	70.7
Galactose	8.4
Glucose	6.7
Ribose	5.8
Maltose	5.1
Fructose	2.8
Xylose	0.6

Alkaloids

Lupinus albus alkaloids are produced in the chloroplasts and then distributed throughout the plant via phloem and stored in the seeds [11] being found in high quantities there. The most common alkaloids present in lupin beans, have a quinolizidine nucleus and exert various biological functions, such as antibacterial [56], antifungal [57] and neurological effects [57]. In the plant, they act as a natural defence mechanism against predators, which can be an advantage because it reduces the necessity to use pesticides that are harmful to the environment, but it is also a disadvantage since they have neurotoxic effects causing tremors, convulsions and excitation [9] only being safe to consume the beans after their removal [12]. Also, when the alkaloids are removed, the seeds are no longer bitter having a more appealing flavour.

Lupinus albus L. produces different types of alkaloids that vary in percentage depending on each species of Lupinus [45]:

- 50-70% lupanine
- 1-3% angustifoline
- 6-15% albine
- 3-10 % multiflorin
- 8-12% 13-Hydroxylupanine
- 1-10% 13-tigloxylupanine
- 0-2% others

It is worth noting that, lupanine is the most abundant alkaloid mainly due to the fact that lupanine is a biosynthetic precursor for other alkaloids [47] being of great interest to the chemical and pharmaceutical industry. In biological organisms, lupanine, inhibits sodium and potassium channels, blocking the transduction of nervous signals [11].

Debittering process

To extract alkaloids from lupin beans, successive extractions with water have traditionally been used (debittering process), since most alkaloids are water-soluble [12]. This process involves the consumption of large amounts of water which is eventually discarded with the effluent wastewater at the end of each leaching batch [16].

The industrial lupin beans debittering process comprises four stages: Swelling, cooking, cooling and extensive washing. During hydration (Phase 1), the lupin beans are left in water for 14 h to swell, then they are boiled (phase 2) inside that same water that was used for phase 1, they are cooled with fresh water and afterwards, the beans are thoroughly washed (phase 4) for around 40 h. Consuming a total of 54 m^3 of fresh water in this last washing step [58]. This process lowers the alkaloid levels to approximately 0.04% and then they can be consumed in human food [12]. At the end of the process, lupin beans can also have a salting phase for preservation.

The amount of lupanine released in each stage of the process is presented in Table 2.2.

Table 2.2: Time, lupanine concentration in the effluent, pH and water spent in each of the different steps of the lupin beans industrial debittering process [58]

Process	**Time**	**pH**	**Luapanine (g/L)**	**Water**
Swelling (Phase 1)	14 hours	7.13	0	0.784 L per Kg of Lupin
Cooking (phase 2)	-	5.7	1.67	water used for swelling is boiled
Cooling (Phase 3)	3 to 4 days	3.89	3.44	1 L per Kg of Lupin
Washing (phase 4)	40 hours	3.8	0.045 - 0.943	between 400 and 1900 L/h

To avoid the extraction of alkaloids, sweet lupin species are grown in various regions of the world. These produce alkaloids in concentrations accepted for consumption, 0.02% of the dry weight of the seed [59]. However, as sweet lupin does not produce alkaloids, it loses its natural defence and it is necessary to use fences and pesticides in order to protect plantations, causing severe environmental problems due to the water and soil contaminations by pesticides [60]. In addition, the sweet lupin comes from a recessive gene, so in the Iberian Peninsula, as the lupin is born spontaneously, due to cross-pollination, it is no longer sweet after a few generations [61].

Lupinus albus has many positive aspects, as a crop it does not require the use of fertilizers and pesticides, can be planted in infertile soils, the root can be sold as natural fertilizer, and the seeds have several uses in the food industry after the extraction of the alkaloids, due to its high nutritional and potential health benefits. Also, after the alkaloids are extracted, they have several applications in the chemical and pharmaceutical industry. However, as a downside, the extraction of alkaloids involves a high expenditure of water and resources.

2.2.3 Membrane filtration's

To reduce some of the amount of water spent in the debittering process, nanofiltration could be used to treat the effluent so it could be reused, as it was first suggested by T. Esteves, et al.[62]. At the same time a retentate, comprising the cooling and the washing phases of the lupin beans industrial debittering process (Table 2.2), is obtained with a lupanine concentration of approximately 3 g/L. This stream is the focus of this thesis for the development of a process for lupanine isolation by adsorption (Figure 2.1) and recovery for further purification and valorisation in the pharmaceutical industry.

The effluent used for the experiments in this study corresponds to phase 3 cooling effluent because it is already at a lupanine concentration of 3 g/L, this is representative of the concentrations of lupanine after the nanofiltration .

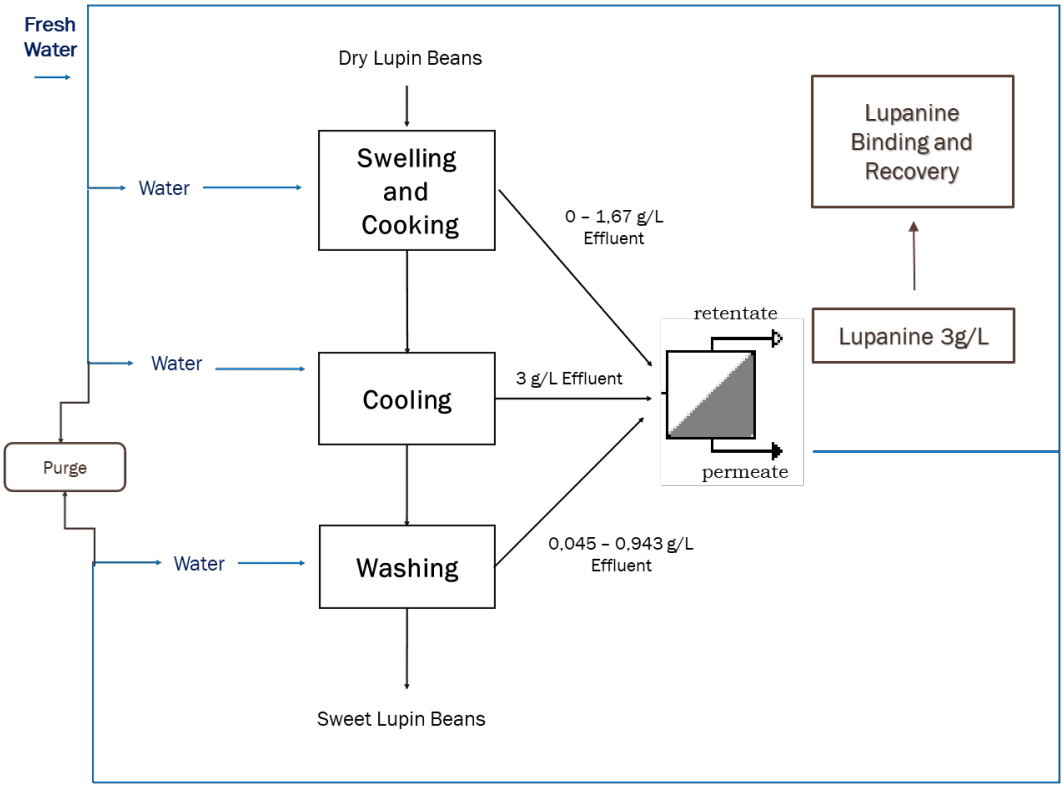

Figure 2.1: Example of a Nanofiltration strategy for lupin beans industrial effluent treatment.

2.2.4 Pharmaceutical properties

Lupin beans have health benefits. The proteins present in the Lupinus albus L. decrease hypercholesterolemia [63, 64] and may also have some anti-inflammatory effects, while lupine hydrolysates may help prevent diseases related to chronic inflammation [65]. Quinolizidine alkaloids from Lupinus species increase insulin secretion, having potential use in the treatment of type 2 diabetes [66].

Also, the lupanine structure includes useful functionalities for the fine chemicals and pharmaceutical industries, serving as a starting material for the synthesis of other alkaloids with high added value [67]. These characteristics make lupanine the main added value compound of Lupinus albus L.

2.3 Bitter Orange

Citrus auratium L. (CA) (Rutaceae), commonly known as bitter orange, as the name suggests has a more bitter albedo and a more acid pulp than other oranges.

It is a fundamental ingredient in many regional cuisines around the world : it is very popular in Afghanistan [68], southern India (used in pachadis, a yogurt-based side dish [68]), China (commonly used as food flavour ingredient [69]) etc. it is also used in the food industry mainly as an aroma and flavour additive used in beverages, marmalade, gelatine, sweets, soft drinks, ice creams, dairy products, oils, candies and cakes [13, 14]. Due to its sour and bitter taste, it has not been much used as an edible fruit [70]. The juice of the fruit is used in salads for sour taste instead of lemon juice [70].

2.3.1 Crop properties

CA can grow in a wide range of soil pH. Although it prefers a pH between 5 and 6, it can grow in the pH range of 4.8 to 8.3 [6] allowing to grow in most of the soils and withstand soil pH changes. Another outstanding characteristic is that it doesn't need manure to grow. In fact, Citrus species dislike it [71].

Although CA best growth occurs within 29-35℃ [5], it is resistant to cold, with the dormant plant being able to withstand temperatures down to about -6℃ [6]. This cessation of growth during winter helps in flower bud induction, resulting in spring flowering but it has no specific requirement of winter chilling, since it thrives well in frost-free sub-tropical to semitropical climate [5].

Even though it can be irrigated, it is unnecessary, since it consumes low amounts of water, as an annual rainfall of 700 mm is sufficient [5]. Actually it should only be irrigated when the compost is almost dry[71] because it is intolerant to water logging[6], so the globally averaged annual precipitation over the land of 715 mm, and in Portugal of 854mm [72] is sufficient. These characteristics show that CA can be a good choice to cultivate food in the future when shifts in temperature and water scarcity will be more severe.

2.3.2 Composition

The chemical composition of the CA includes vitamins, minerals, phenolic compounds such as flavonoids, amines, among others [15]. Citric acid is the most abundant organic acid in CA, corresponding to 97% of all organic acids present in bitter orange juice [70] (Table 2.3). In the peel, the most predominant organic acid was found to be the oxalic acid corresponding to 54% of total acids [70]. As we can see in Table 2.3 there are other acids present in CA juice such as oxalic acid, malic acid, and ascorbic acid. In the peel other organic acids present are quinic acid and ascorbic acid [70].

Table 2.3: Organic acid content of CA samples. Data from: [70]

Sour Orange	Oxalic	Malic	Ascorbic	Citric	Quinic
Juice (mg/L)	89.5±2.4	384.6±12.9	312.2±19.7	39153.3±328.8	n.d.
Peel (mg/100 g)	257.5±25.3	N.d	117.6±7.3	n.d.	98.5±10.4

Naringin and Hesperidin

Flavonoids are some of the major bioactive constituents of bitter orange fruits, such as naringin, hesperidin, neohesperidin, naringenin and hesperetin. The characteristics of these flavonoids have been investigated intensively, and they have shown to possess antioxidant [73], antiviral, anti-allergic [74],

vasoprotective [75] and anticarcinogenic properties [75]. CA extract also showed potential pesticidal activity [76].

Naringin and hesperidin (Figure2.2) are the most abundant flavonoids in CA reaching a concentration of 299.2 ± 0.5 mg/kg and 210.3 ± 1.3 mg/kg of dry fruit, respectively [77].

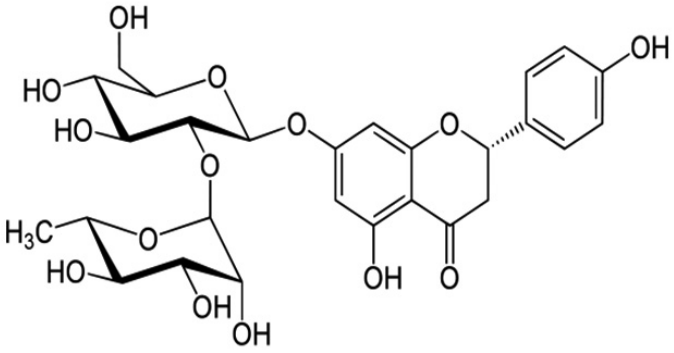

Naringin

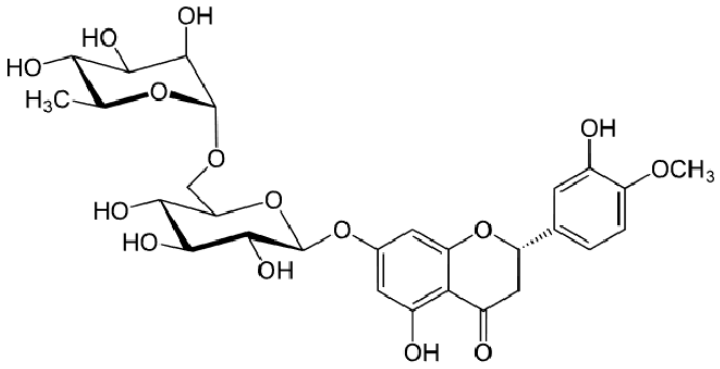

Hesperidin

Figure 2.2: Chemical structure of naringin and hesperidin

The poor aqueous solubility of hesperidin limits its dissolution rate in water, which finally results in poor *in vivo* bioavailability [78]. Hesperidin has also been reported as insoluble in most of the physiologically safe organic solvents like ethanol, so in most studies, it has to be extracted with methanol, where it shows to be very soluble [78].

Naringin concentration in bitter orange increases when the fruit matures, while, hesperidin, on the other hand, diminishes [79].

The total phenolic content and total flavonoid content of the bitter orange peel is higher than in other commonly used citrus fruit peels such as lemon, orange, and grapefruit [70], making bitter orange a great source to obtain these compounds.

Table 2.4: Total phenolic and total flavonoid content of sour orange samples. Data from:[70] . Concentrations in GAE (Gallic Acid Equivalence) a colorimetric assay using Folin-Denis reagent.

	Juice (GAE/100 mL)	Peel (GAE/100 g)
Total Phenolic Content	56.9±2.4	487.1±5.1
Total Flavonoid Content	7.7±0.8	387.4±6.9

Synephrine

Other bioactive compounds commonly found in citrus Aurantium are the amines with adrenergic activity such as octopamine, tyramine, N-methyl-tyramine, hordenine, and synephrine (Figure 2.3), with the last one being the most abundant amine in CA [46].

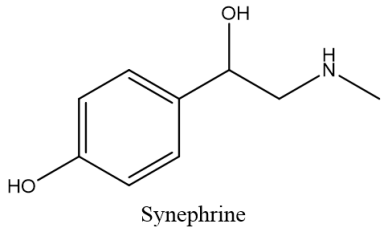

Figure 2.3: Chemical structure of synephrine

Synephrine is naturally present in citrus plants. It is a sympathomimetic alkaloid that exists in three different positional isomers (ortho *o*-, meta *m*-, and para *p*-). However, only *p*- and *m*-synephrine have been described in weight-loss products [48].Synephrine acts on several adrenergic and serotonergic receptors and has activity on trace-amine-associated receptors [80]. This adrenergic stimulation results in weight loss [81].

Some authors argue that both *p*- and *m*-synephrine are present in CA fruits [82, 83], but most literature describes only *p*-synephrine to be present [82-84]. Its use became popular after the US Food and Drug Administration (FDA) prohibited the use of ephedrine-containing dietary supplements, because these products increase blood pressure exposing users to serious adverse events such as stroke, heart attack, and death [84]. Due to the structural similarities between ephedrine and p-synephrine, it has been assumed a similar pharmacological effect of p-synephrine to those of ephedrine, without the contraindications found for the last one [15]. The consumption in the form of CA extract and as pure synephrine at therapeutic doses was proven to have no unwanted effects in animals and human models [15].

2.3.3 Pharmaceutical properties

CA was traditionally used as a medicinal material in China because of its various pharmacological activities [85], with multiple therapeutic potentials, such as [15]:

- Anticancer: Flavonoids extracted from CA have potential chemotherapeutic properties against cancer [86]. They mediate the inhibition of several kinases (kinase inhibitors) which are involved in cell-cycle arrest and cell apoptosis. This inhibition will vary depending on the structure of each flavonoid [75], each acting in different development stages of malignant tumours [87].
- Antianxiety: Preparations of citrus aurantium L. (Rutaceae) are popularly used in order to minimise central nervous system disorders [88]. CA essential oils showed sedative activity effects in mice, after a single treatment [89].
- Antiobesity: Flavonoid-rich extracts from CA, comprising 32.15% of neohesperidin, hesperidin and naringin, showed anti-obesity effects in mice [90]. Synephrine present in CA showed promising results in the treatment of obesity by increasing energy expenditure, increasing metabolism, and suppressing appetite [83].
- Antibacterial: Citrus aurantium juice presented antibacterial effects on Salmonella Typhimurium and Listeria monocytogenes after 7 days of incubation, although it was found that the antimicrobial effect of sour orange juice mainly depended on its low pH value [91].

- Antioxidant: CA flavonoids (naringin, naringenin and hesperidin) were reported to impair reactive oxygen species, having antioxidant action protecting against oxidative stress linked to inflammation and reducing the risk of macromolecule damage caused by free radicals [73].
- Antidiabetic activity: Neohesperidin derived from CA significantly elevated oral glucose tolerance and insulin sensitivity and decreased insulin resistance in the diabetic mice showing great potential in the prevention of diabetes [92].

2.4 Added Value Compounds Extraction

Lupanine and synephrine present in lupin beans and bitter orange, respectively, are toxic for human consumption (at concentrations above the therapeutic dosage) . To use lupin beans and bitter orange in food production, it is necessary to reduce the concentration of these two alkaloids. Many unit operations can be used to extract alkaloids from solutions, such as filtration, liquid-liquid extractions, adsorption methods, etc.

Membrane separations are also some of the most used choices for separation processes mainly because of their simple process scale-up, low energy use and lack of necessary chemical additions, but they lack selectivity and it's necessary to further process the resulting streams to isolate the added value compounds desired. The same issues apply to liquid-liquid extractions, besides having a high environmental impact, by the production of a huge amount of solvent waste, they also lack selectivity and further processing is needed.

Although the processes mentioned above could be efficient in extracting the alkaloids from the effluent of lupin beans and the orange juice allowing their consumption, further processing is needed to isolate and purify them. The most appropriate processing methods that can extract these compounds with higher selectivity are adsorption separation methods, such as the use of commercial resins or polybenzimidazole (PBI).

Adsorption methods are the most used to treat wastewaters [93], and the most common procedures used to separate and purify alkaloids from plant materials are the use of precipitation, ion exchange resins, adsorption resins and silica gel. Resins are cheaper and have lower operating pressure (when used as columns) than silica gel, they are more suitable for the preliminary separation of alkaloids [94]. In this way, it is possible to extract and isolate the added value compounds for further valorisation, in the chemical and pharmaceutical industries, in a simpler way with a more environment-friendly technique with high efficiency and lower toxicity.

2.4.1 Resins

Synthetic resins are used in water and wastewater treatment, food processing and medicinal applications. They form an integral part of many food processing units, mainly for the removal of unwanted compounds [95]. Commercial resins are not expensive, do not require complicated procedures and are commonly used in adsorption separation processes because of their hydrophobicity or ionic selectivity [96, 97]. Also, one of the main advantages of using resins is that they can be reused upon regeneration [98].

Resins are classified into two types: ion exchange resins or polymeric adsorbents. Ion exchange resins act based on the interchange of ions between two phases, the insoluble phase (the resin) and the solution phase [96, 99].

The insoluble phase contains immobilised acid groups (cation exchange resins Y^-) or base groups (anion exchange resins X^+) that exchange positive or negative counter ions (A^- or C^+) [96, 99], as

demonstrated in Figure 2.4. Ionic exchange resins are commonly used for pharmaceutical production, fine chemical processing and food processing.

With polymeric adsorbents, the interactions between the compounds and the resin are based on hydrogen bonding, hydrophobic or van der Waals interactions [97]. Comprising many different polymer formulations, polymeric adsorbents are stable at virtually all pH levels, which allows operation in conditions under which silica-based materials are unsuitable.

Alkaloids, also known as organic bases, are widely distributed in many plant materials, and most of them have significant physiological activities. Its alkalinity can be characterised by the value of its conjugated acid pKa (synephrine has a pKa of 9.8 [100] and lupanine has pka of 9.1 [101]).

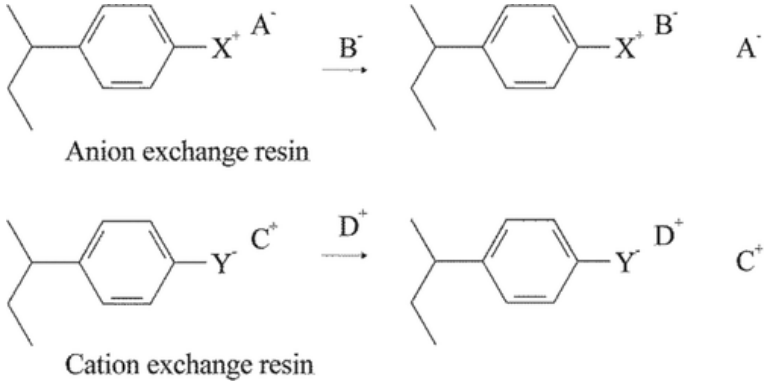

Figure 2.4: Example of polystyrene – based anion and cation exchange resins [99]

Both compounds are present in acidic solutions (the lupin beans process effluent [58] and the bitter orange juice) which means that these compounds will be present as ions, with a positive charge. Based on this, the best resins for the isolation of these compounds would be the cationic exchange resins [62]. The positive charge of lupanine and synephrine will exchange with the protons of the sulphonic or carboxylic acid groups depending on the type of the cationic resin [98].

Moreover, because we are considering two organic compounds, the polymeric adsorbers will also be a good possibility. These resins will interact through hydrophobic and polar effects with the compounds due to their aromatic bonds [98], as observed for lupanine and the resin Amberlite XAD-16 [62].

Not only is necessary to have good adsorption capacities, but the resin should also allow the highest possible recovery percentage of the desired compounds. For example, if a resin binds 100% of the compound of interest from the solution but it's not possible to recover it from the adsorber, we cannot further isolate it. So, a strong acid cation exchanger, that has a strong affinity to alkaloids, might not be the best choice, but rather a weak acid cation exchanger that can bind the alkaloids but can allow us to recover most of it from the resin and re-use the resin making the extraction more efficient [62, 98].

These are theoretical approximations; each alkaloid is present in a complex mixture (the industrial effluent and the bitter orange juice) that can influence the way the alkaloids will bind to the functional group of each resin. Therefore, two resins of each type were selected to assess preferential binding to synephrine or flavonoid compounds in citrus orange juice: cation exchange (AG50W-X8 and Purolite PD206), anion exchange (Amberlite IRA-68 and Amberlite IRA-458) and polymeric adsorbent (Amberlite XAD-16 and Amberlite XAD 4). The characteristics of these resins are presented on Table 2.5.

Table 2.5: Resin classification, Particle size, structure of the matrix, functional groups and Ionic forms for each of the resin tested.

Resin	Classification	Particle size	Matrix	Functional group	Ionic Form
AG 50W-X8	Strong acid cation Exchange	160-250 μm	Polystyrene cross-linked with 8% divinylbenezene	Sulfuric acid	Hydrogen (H+)
PUROLITE PD206		300-120 μm	Polystyrene cross-linked with divinylbenzene		
IRA 68	Weak base anion echange	595- 841 μm	Crosslinked acrylate	Tertiary ammonium	Free base
IRA 458	Strong base anion exchange	700-1000 μm	Polyacrylic	Quaternary ammonium	Chloride
XAD 16	Polymeric Adsorbent	560-710 μm	Hydrophobic polyaromatic	NA	NA
XAD 4		490-690 μm			

2.4.2 Polybenzimidazole (PBI)

Polybenzimidazoles (PBI, Figure 2.5) is an extremely heat-resistant heterocyclic thermoplastic that is being used for various applications, in particular, for high-temperature applications, fibre spinning, and reverse osmosis and organic solvent nanofiltration membranes (allowing high-temperature filtrations [102]), because of its excellent thermal and chemical tolerance and film-forming capability [103].

PBI has a pka of 5.5 [104] and proton donor (-NH-) and a proton acceptor (-N=) hydrogen-bonding sites (Figure 2.5) which exhibit specific interactions with protic and aprotic polar solvents [105]. PBI has been subject to some modifications (structural and ionic) and its adsorption potential has been assessed for the removal of genotoxic impurities from solutions containing active pharmaceutical ingredients [106]. In these studies, the following modifications were performed:

- PBI with thermal treatment (PBI-T) : raw PBI was dissolved in Dimethyl sulfoxide (DMSO) at high temperatures ($>$ 160 ^{o}C), and precipitated with water to increase the surface area of the polymer.
- PBI with thermal and acid treatment (PBI-TA) : PBI-T was conditioned with hydrochloric acid (HCl) to induce ionic interactions between the polymer and the adsorbate.
- PBI with thermal and basic treatment (PBI-TB) : PBI-T was conditioned with sodium hydroxide (NaOH) to induce ionic interactions between the polymer and the adsorbate.

The synthesis and processing of active pharmaceutical compounds are usually carried out in organic solvents, so PBI is an interesting polymer because it is compatible with these solvents. The purification of lupanine is also interesting for the same reason, although the adsorption process with PBI will be performed in an aqueous solution (effluent) the recovery process can be performed using organic solvents, allowing to explore, if necessary, harsher chemical conditions and organic solvents. This is something that cannot be done with commercial resins.

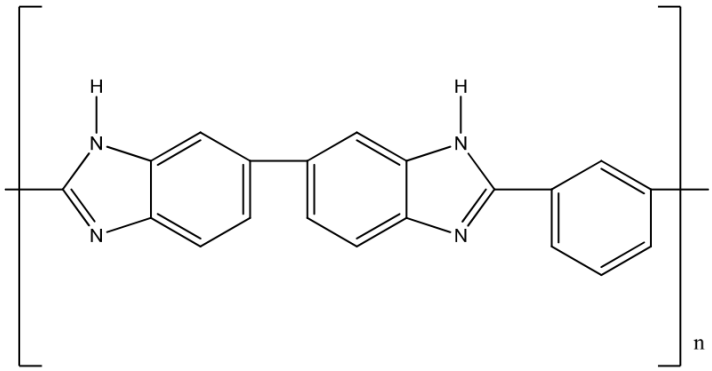

Figure 2.5: PBI Molecular Structure [103]

2.4.3 Adsorption modeling methods

Modeling the experimental data from the adsorption processes can help us predict the mechanisms of the various adsorption systems and design low-cost adsorbents for the detoxification of effluents [107]. Having a good interpretation and understanding of the adsorption equilibrium information is the most important piece of information needed to improve the adsorption mechanism pathways and effectively design the adsorption process [108].

2.4.3.1 Adsorption isotherms

Adsorption isotherms are used to describe the equilibrium relationships between adsorbent and adsorbate. The linear regression analysis has been one of the most applied tools for defining the best fitting adsorption models, but with the evolution of computer technology, there has been an increase in the use of nonlinear isotherm modelling [108].

Adsorption isotherms linear regressions usually correlate the quantity adsorbed and that remaining in solution at a fixed temperature [107]. There are many forms of adsorption isotherms,the methods most widely used, and are two of the oldest isotherms, are the Freundlich and the Langmuir models. Both models are often used at the same time to compare and choose the better one according to the determination coefficient (R^2) [94]. The Freundlich isotherm can be used for non-ideal adsorption on heterogeneous surfaces and the Langmuir isotherm assumes monolayer adsorption on a homogenous surface [107].

There are other simpler Isotherm models that are not as widely used such as Henry's isotherms (a one-parameter isotherm model) but because it only has an appropriate fit at relatively low concentrations of adsorbate, considering that all adsorbate molecules are secluded from their nearest neighbours [108] it wasn't tested for our adsorptions.

2.4.3.2 Adsorption kinetic equations

Adsorption kinetics measures the rate of adsorption, which determines the time required to reach equilibrium for the adsorption process [109].The type of adsorption and the accessibility to adsorption site will influence the adsorption kinetics.

Although we refer to adsorption as one step, it involves several steps that affect the kinetics. The first step of adsorption is bulk diffusion (when the adsorbate goes from its original solution to near the liquid surrounding the solid adsorbent). The second step is the external diffusion (when the adsorbate has to cross the liquid that is surrounding the solid adsorbent particles), subsequently, it enters the adsorbent

particles through interparticle diffusion and finally there is the interaction with the surface sites. For the case of reversible adsorption, there is also the desorption of the adsorbate from the adsorbent surface. The overall rate of the adsorption is controlled by the slowest of the above steps [109].

The adsorption rate is an important index when optimising the resin for absorbing alkaloids . There are a variety of different models to fit the adsorption rates. These models describe the rate of retention of adsorbate from a solution to the solid-phase interface at a given adsorbent dose, temperature, flow rate and pH [110].

The pseudo-first-order and pseudo-second-order kinetic models are the most commonly used empirical models for alkaloid adsorption [94].

The pseudo-first-order kinetic model, also known as the Lagergren model, is more accurate to fit, the initial stage of adsorption, for a high initial concentration of adsorbate. When the initial concentration is low, the pseudo-second-order kinetic model is more suitable for fitting the subsequent stage of adsorption [94]. The mixed order model is a mix of the above-described models, and it can fit the whole adsorption process of any initial concentration [94]. Elovich model (developed by Zeldowitsch) helps to predict the mass and surface diffusion, activation and deactivation energy of a system. This model often is applied in gaseous systems but it also is applicable in some effluent processes. It assumes that the rate of adsorption of solute decreases exponentially as the amount of adsorbed solute increases [110].

Chapter 3

Methods and Materials

3.1 Materials

Reagents Ethyl acetate (EtOAc), tetrahydrofuran (THF),isopropanol (IPA), Ethanol (EtOH), Hexane, dichloromethane (DCM), methanol (MeOH),glacial acetic acid (AcOH) and acetonitrile (MeCN) HPLC-grade, HCl 37% solution,potassium hydroxide (KOH) pellets and NaOH pellets were purchased from Fischer Scientific. DMSO was purchased from Carlo Erba Reagents S.A.S and 1-Butanol was purchased from Merck KGaA.

Bovine serum albumin (BSA), Coomassie Brilliant Blue and 3,5-Dinitrosalicylic acid was purchased from Merck KGaA. Dowex AG50W-X8 was purchased from BDH Chemicals Ltd Poole England; Purolite PD206 was purchased from Purolite ion exchange resins; Amberlite IRA68, Amberlite XAD-4 and Amberlite IRA458 were purchased from Rohm and Haas France S.A.S; Amberlite XAD-16 was purchased from ThermoFisher (Kandel) GmbH.

Hesperidin (CAS 520-26-3) and Synephrine (CAS 94-07-5) were purchased from TCI Chemicals Europe N.V and Naringin (CAS 10236-47-2) was purchased from Alfa Aesar.

Pristine polybenzimidazole (PBI) polymer 100 mesh powder was purchased from PBI Performance Products Inc. (USA).

Raw materials Industrial lupin beans effluent, with a lupanine concentration of 3 g/L (debittering phase), was kindly provided by Tremoceira M. Ferreira Bastos Lda. (TMFB) Portugal. This effluent with this lupanine concentration was chosen as a representative of the concentrations of lupanine after the nanofiltration process.

Lupanine was kindly provided by the Faculty of Pharmacy of the University of Lisbon.

Mature bitter orange fruits were collected at Instituto Superior Tecnico (IST) Alameda, Lisbon, Portugal in 2020 (16 of December).

Equipment The reagents and materials were weighted using an analytic balance (Sartorius, CPA64 d=0.1mg). To measure absorbances required to perform Bradford and DNS methods, and to register UV Spectrum (200 - 400 nm) of Naringin, Hesperidin and Synephrine, a Microplate reader (Multiskan Go Microplate Spectrophotometer) was used.

Quantification of lupanine was performed on a Hitachi LaChrom High Performance Liquid Chromatography (HPLC) with a Kinetex 5 µm EVO C18 100A LC column (250 mm x 4. 6mm). The HPLC was constituted by two pumps (L-7100), an interface module (D-7000), an autosampler (L7250) and a

UV detector (L-7400, =220 nm).). The mobile phase consisted of 15% of MeCN and 85% of aqueous Na_2HPO_4 buffer (pH 10.5) at a flow rate of 1 mL/min, injection volume of 20 µL and 30 min of run time.

The detection of sugars and organic acids in the effluent was performed using a Hitachi LaChrom Elite HPLC equipped with a Rezex ROA-Organic acid H+ 8% (300 mm x 7.8 mm) column, an autosampler (L-2200), a L-2130 pump, a L-2490 refraction index (RI) detector for sugars and phosphate and a Hitachi L-2420 UV-Vis detector for organic acids. The injection volume was 20 µL, with a flow rate of 0.5 mL/min and elution was achieved using a 5 mM solution of H_2SO_4 as mobile phase. The column was kept at 65 ℃ under a pressure of 26 bar and 30 min of run time .

Quantification and detection of synephrine, naringin and hesperidin were performed on a VWR Hitachi Chromaster HPLC equipped with a Luna 10 µm C18(2) 100 A , (250 mm x 4.6 mm) LC Column, a UV-Vis Detector (5420), a Column Oven (5310) and na autosampler (5260). For synephrine and naringin in the bitter orange juice synthetic mixture the UV detection was 225nm for synephrine and 283 nm for naringin, the injection volume was 10 μL, with a flow rate of 1 mL/min and the mobile phase consisted of 50%Water (0.6% acetic acid) and 50% Methanol and 27 min of run time. For synephrine, naringin and hesperidin on bitter orange dried extracts the UV detection was 225 nm, the injection volume was 10 μL, with a flow rate of 0.6 mL/min and the mobile phase consisted of 60%Water (0.6% acetic acid) and 40% Methanol and 60 min of run time.

Bitter Orange samples were lyophilised on a CHRIST Alpha 1-2 LD plus lyophilizer.

The Bitter orange fruits were dried in a Vacuum Drying Oven Heraeus Vacutherm VT 6025 (Thermo scientific) at 40^{o}C under a pressure of 100 mbar and grinded on a Moulinex original grinder

3.2 Methods

3.2.1 Lupin beans effluent characterization and membranes

3.2.1.1 Sugars and organic acids

Acid hydrolysis [111]

Sulfuric acid hydrolysis was used to hydrolyse the polymeric forms of carbohydrates present in the effluent into monomeric subunits. To do that, 143.75 ml of effluent were mixed with 6.25 ml of H_2SO_4 for a final concentration of H_2SO_4 of 4% (w/w). Then, this mixture was placed in a borosilicate glass bottle, and it was autoclaved for 1 h at 121 ℃. After completion of the autoclave cycle, the sample was allowed to cool down to room temperature.

After this, the mixture was vortexed, and a 3 mL aliquot was taken into a 50 mL Erlenmeyer flask for pH adjustment (pH 5.5) with calcium carbonate added in small amounts, with vortex between additions, allowing the sample sufficient time to finish bubbling before checking the pH. Calcium carbonate, if added in large amounts, often leads the sample to froth and turn into a lump of precipitate. It is very important to adjust the pH of the sample correctly as low and high pH values can damage the HPLC column [111], including, but not limited to, aliquot amount and sample buffering capacity. As the neutralisation process progresses is normal to form a precipitate in the sample. Aliquots are typically about 1–3 mL and large volumes of hydrolysate should not be neutralised at once. Also, the vessel must be large enough to contain the sample when it off-gases and bubbles during the neutralisation process.

HPLC sample preparation

Three different samples derived from the effluent were analysed in the HPLC: the standard effluent, a basified sample of the effluent and the effluent obtained after hydrolysis. 1ml of each sample was centrifuged, and the supernatant was filtered through a 0.2 µm nylon filter. Samples for HPLC analysis

were prepared by mixing 400 µL of each sample with 1600 µL of a 50 mM solution of H_2SO_4 in a microtube, giving a final dilution of 1:5. Each sample was prepared as follows:

1. **Standard Effluent:** the effluent has a pH of 4 so it was basified with calcium carbonate to a pH of 5.5.
2. **Basified Effluent:** the effluent was basified with 1 pellet of KOH reaching a pH of 14 that caused precipitation of some impurities ,the impurities were filtered, and the pH of the sample was adjusted to 8 with the addition of H_2SO_4 50 mM.
3. **Hydrolysed Effluent:** this sample was obtained applying the procedure described in the previous section.

3.2.1.2 Total protein- bradford assay

The Bradford protein assay was used to determine the total protein concentration of the effluent. This method is based on the proportional binding of the dye Coomassie to proteins. It is a colourimetric method. As the protein concentration increases, the colour of the test sample becomes darker. Coomassie absorbs at 595 nm. The protein concentration of a sample is compared to a series of protein standards (the protein used as a standard was Bovine Serum Albumin (BSA) [112] and then determined. The concentration is determined by the Lambert-Beer law (equation. 3.1), where A is the absorbance, ε is the molar attenuation coefficient or absorptivity of the attenuating species, ℓ is the optical path length in cm and c is the concentration of the attenuating species.

$$A = \varepsilon \ell c \tag{3.1}$$

- Calibration curve preparation:
  1. Mix 25 mg of BSA in 25mL of water (standard solution).
  2. Do test solutions for the reference standards according to Table 3.1.
  3. Shake vigorously in a vortex.
  4. In a 96 well plate add 196µL of coomassie + 4µL standard solution. It is important to make a blank too (196µL of coomassie + 4µL of water).
  5. Wait 2 min and read the absorbance at 595 nm using a microplate spectrophotometer.
  6. Plot the absorbance of each standard solution as a function of its theoretical concentration (Figure A.2). The plot should be linear. Use the obtained equation to calculate the concentration of the protein sample based on the measured absorbance.

Table 3.1: BSA Standard solutions for Bradford Calibration curve preparation

Water (mL)	Standard solution (mL)	Concentration (mg/mL)
1	0	0
0.9	0.1	0.1
0.8	0.2	0.2
0.7	0.3	0.3
0.6	0.4	0.4
0.5	0.5	0.5

- Determination of protein concentration in the sample:

1. In a 96 well plate add 196 µL of coomassie + 4 µL of sample. It is important to make a blank too (196 µL of coomassie + 4 µL of water).
2. Wait 2 min and measure the absorbance at 595 nm using a microplate spectrophotometer.
3. Use the calibration curve to obtain the protein concentration.

3.2.1.3 Total reducing sugar- DNS assay

The 3,5-dinitrosalicylic acid (DNS) is reduced to 3-amino-5-nitrosalicylic acid by glucose (containing hydroxyl groups, -OH). The reduced DNS is a coloured compound that absorbs light with a wavelength of 540 nm, so it's possible to establish a direct relationship between the colourimetric measurement and the amount of reducing sugars in the sample making this spectrophotometric analysis a reliable, robust, and simple method [113].

- Calibration curve preparation:
  1. Do test solutions for the reference standards according to Table 3.2.
  2. Shake vigorously in a vortex.
  3. In a 96 well deep plate add 100 µL of DNS + 100 µL of standard solution. It is important to make a blank too (100 µL of DNS + 4 µL of water).
  4. Cover the 96 well deep plate with aluminium foil and incubate at 100 ℃ for 5 min.
  5. Let it cool to room temperature, add 500 µL of distilled water and shake.
  6. Transfer 200 µL of each well into the corresponding well of a 96 well plate.
  7. Measure the absorbance at 540 nm using a microplate spectrophotometer.
  8. Plot the absorbance of each standard solution as a function of its theoretical concentration (Figure A.3.) The plot should be linear. Use this equation to calculate the concentration of the protein sample based on the measured absorbance.

Table 3.2: Glucose standard solutions - DNS calibration curve preparation

Water (mL)	Standard solution (mL)	Concentration (mg/mL)
1	0	0
0.9	0.1	0.1
0.8	0.2	0.2
0.7	0.3	0.3
0.6	0.4	0.4
0.5	0.5	0.5
0.4	0.6	0.6
0.3	0.7	0.7
0.2	0.8	0.8
0.1	0.9	0.9
0	1	1

- Determination of reducing sugars in the samples:
  1. In a 96 well deep plate add 100 µL of DNS + 100 µL of sample solution. It is important to make a blank too (100 µL of DNS + 4 µL of water).
  2. Cover the 96 well deep plates with aluminium foil and incubate at 100 ℃ for 5 min.

3. Let it cool to room temperature, add 500 µL of distilled water and shake.
4. Transfer 200 µL of each well into the corresponding well of a 96 well plate.
5. Measure the absorbance at 540 nm using a microplate spectrophotometer.
6. Convert the optical density values for reducing sugar concentrations based on the calibration curve.

3.2.1.4 Lupanine quantification and calibration curves

A stock solution of lupanine was prepared by dissolving 0.1 g of pure lupanine in 10 mL of Milli-Q water (10 g/L). Aliquots of the stock solution were pipetted in consecutive dilutions into 14 volumetric flasks to obtain solutions of lupanine with concentrations between 10 g/L and 0.005 g/L (Table 3.3)

Table 3.3: Lupanine consecutive dilutions

Lupanine (g/L)	Volume from the stock solution (μL)	Final Volume (mL)
10	0	10
7.5	7500	10
5	5000	10
4	4000	10
3	3000	10
2.5	1250	5
1	500	5
0.5	250	5
0.25	150	5
0.1	250	10
0.05	125	25
0.025	125	25
0.01	50	50
0.005	50	100

A 1.5 mL sample of the solutions with different lupanine concentrations was transferred to HPLC vials for HPLC analysis. The calibration curve was then obtained by plotting the area of the lupanine peak as a function of the concentration (Figure A.4).

For lupanine quantification the effluent samples were basified with KOH (pH 14), centrifuged using a micro-centrifuge (Sigma) at 10,000 rpm for 3 min and filtered with nylon syringe filters (13 mm diameter and 0.22 µm pore size, Tecnocroma) and transferred to HPLC vials. Then, the lupanine calibration curve (Figure A.5 and Figure A.6) was used to obtain the lupanine concentration in the samples.

3.2.1.5 Membrane filtration

100 ml of previously basified lupin beans effluent (lupanine 3 g/L) of effluent was concentrated using a NF270 (from Dow FILMTEC) nanofiltration membrane. The conditioning of the membrane was done by adding 200 mL of distilled water into the filtration cell under a pressure of 15 bar until a constant flux was obtained. Then the 100 ml of basified efluent was placed in the feed tank. 50 mL was filtered and 50 mL of effluent was left in the retentate.

3.2.2 Lupanine adsorption experiments

3.2.2.1 PBI derived adsorbers

PBI thermal treated (PBI-T) [106] : Was obtained by dissolving pristine PBI polymer in DMSO (15% w/w) by heating, under air, at 163 ℃ for 3 h with magnetic stirring and further 100 ℃ for 24 h. The solution was then cooled to 50 ℃ and precipitated with water (Figure A.7). The resulting solid was crushed, filtered, and successively washed with water (40 mL/g polymer), MeOH (20 mL/g polymer) and DCM (20 mL/g polymer) for 3 min each with magnetic stirring (3 times for each solvent). The solid obtained was then dried under vacuum.

Ph Conditioning [106] : PBI-T was pH conditioned with HCl 0.25 M (PBI-TA) or NaOH 0.1 M (PBI-TB) solutions by washing. The polymers were immersed for 3 min in 20 mL of acidic or basic solution per gram of polymer with magnetic stirring. After this, the polymers were successively washed by magnetically stirring for 3 min in solutions of water (40 mL/g polymer), MeOH (20 mL/g polymer) and DCM (20 mL/g polymer) (3 times for each solvent) and dried under vacuum overnight.The polymers were removed from each solution by simple filtration and transferred to the next solvent.

3.2.2.2 Lupanine binding assessment

Binding assays were performed by adding to 2 mL Eppendorf tubes, 100 mg of each PBI polymer, and 1 mL of solution (1 mL of lupanine stock solution at 3g/L or lupin beans effluent regular pH or basified). The tubes were allowed to stand overnight at room temperature, under agitation (100 rpm) with magnetic stirring. Each polymer was tested in duplicate. After this, the tubes were centrifuged at 10,000 rpm for 3 min, and the supernatant was recovered and basified with KOH pellets (pH between 13 - 13.5). After this, the samples were centrifuged again, at 10,000 rpm for 3 min and the supernatant was filtered to HPLC vials and analysed for lupanine quantification. Duplicate samples of the stock solutions (pure lupanine and effluent) were also analysed by HPLC for lupanine quantification. The effluent sample was processed as previously described.

The lupanine calibration curve (Figure A.5 and Figure A.6) were used to obtain the lupanine concentration in the samples.

The percentage of lupanine bound to the adsorbers was calculated from equation 3.2 where C_0 (mg/L) is the initial lupanine concentration and C_f (mg/L) is the final lupanine concentration in solution.

$$\text{binding } (\%) = \frac{[C_0 - C_\text{f}]}{C_0} \times 100 \tag{3.2}$$

The adsorption capacity of each adsorber was calculated from equation 3.3 where Q (mg/g) is the amount of lupanine bound to the adsorber, C_0 (mg/L) is the initial lupanine concentration, C_f (mg/L) is the final concentration of lupanine in solution, V (L) is the volume of solution used, and M (g) is the adsorber mass.

$$Q = \frac{V \times [C_0 - C_\text{f}]}{M} \tag{3.3}$$

3.2.2.3 Binding adsorption isotherm experiments

Binding adsorption isotherm experiments were performed at room temperature. 1 mL of basified effluent was added to different amounts of PBI-T, from 10 mg to 100 mg. The mixtures were left overnight stirring at 100 rpm under magnetic agitation. The experimental data were fitted to Langmuir (equation 3.4) and Freundlich (equation 3.5).

$$\frac{q_{\mathrm{e}}}{q_{\mathrm{m}}} = \frac{K_{\mathrm{L}} C_{\mathrm{e}}}{1 + K_{\mathrm{L}} C_{\mathrm{e}}} \tag{3.4}$$

$$q_{\mathrm{e}} = K_{\mathrm{F}} C_{\mathrm{e}}^{1/n} \tag{3.5}$$

Where q_e (mg/g) is the amount of compound bound to the adsorber in a monolayer and q_m (mg/g) is the maximum amount of compound bound to the adsorber in a monolayer for the Langmuir model, whereas K_L and K_F are equilibrium constants (L/mg) for the Langmuir and Freundlich models, respectively, and n is a parameter related with the surface layer heterogeneity [114].

The values of the parameters K_L (Langmuir equilibrium constant (L/mg)) and q_m (maximum amount of compound bound to the adsorber in a monolayer) of the Langmuir Isothem model can be obtained by the linearization of the equation 3.4, obtaining equation 3.6:

$$\frac{C_e}{q_e} = \frac{1}{q_m} C_e + \frac{1}{k_L q_m} \tag{3.6}$$

The values of the parameters K_f (Freundlich equilibrium constant (L/mg)) and n (parameter related with the surface layerheterogeneity) of the Freundlich isotherm model can be obtained by the linearization of equation 3.5, obtaining equation 3.7 :

$$\ln(q_e) = \left(\frac{1}{n}\right) \ln(C_e) + \ln(K_f) \tag{3.7}$$

3.2.2.4 Binding kinetics experiments

Binding kinetics experiments were performed at room temperature for 100 mg of PBI-T and 1mL of basified effluent, left stirring at 100 rpm and collected after certain time intervals (2, 5, 10, 15, 60, 120, 180, 240, 360, 420, 1380, 1440 and 1620 min).

The experimental data were fitted to pseudo first- and pseudo-second-order kinetic models equation 3.8 and 3.9 respectively:

$$\ln(q_e - q_t) = \ln(q_e) - k_1 t \tag{3.8}$$

$$\frac{t}{q_t} = \frac{1}{k_2 \cdot q_e^2} + \frac{t}{q_e} \tag{3.9}$$

Where q_e and q_t (mg/g) are the adsorption capacities at equilibrium and at time t (min), respectively, and k_1 (min^{-1}) and k_2 (g/ (mg·min)) are the pseudo-first-order and second-order rate constants for the models [114].

3.2.2.5 PBI-T efficiency assay

PBI-T efficiency assays were performed by adding to 100 mg of PBI-T polymer different volumes of Basified Effluent (1 mL; 2 mL; 5 mL; 10 mL ; 15 mL ; 20 mL ; 40 mL)) under magnetic agitation (100 rpm) for 17h.

Alternatively, binding assays were performed by adding to 2 mL Eppendorf tubes, 100 mg of PBI-T polymer, and 1 mL of lupin beans effluent at different concentrations of lupanine (previously diluted with water from the concentrated effluent). The tubes were magnetically agitated (100 rpm) for 17 h at room temperature. After this, the tubes were centrifuged at 10,000 rpm for 3 min, and the supernatant was recovered and basified with KOH to a pH between 13 - 13.5 and analysed for lupanine quantification in HPLC.

3.2.2.6 Saturation assay

Saturation assays were performed by adding to 2 mL Eppendorf tubes, 100 mg of each PBI polymer, and 1 mL of basified effluent. The tubes were magnetically agitated (100 rpm) for 17 h at room temperature. After this, the tubes were centrifuged at 10,000 rpm for 3 min, and the supernatant was recovered and basified with KOH to a pH between 13 - 13.5 and analysed for lupanine quantification in HPLC, the pellet was re-suspended in the basified effluent and the process was repeated 3 times.

3.2.3 Lupanine recovery assays

After binding experiments, it was added 1 mL of each recovery solvent to the PBI pellet. The re-suspended mixture was left at 100 rpm at room temperature for 24 h. After this time, the mixtures were centrifuged at 10,000 rpm for 3 min for PBI separation. The organic solvents were evaporated at room temperature and the volume was refilled with water and basified with KOH (pH between 13 - 13.5) before the lupanine HPLC analysis protocol.

Recovery solvents tested on all different PBI: HCl 0.1M, MeOH HCL 0.1M, DCM, EtOH, THF, and Ethyl acetate. Recovery solvents tested only for PBI-T: Water (also tested at 50 ^{o}C), HCL 1M (also tested at 50 ^{o}C), NaOH 1M (also tested at 50 ^{o}C), Butanol, Isopropanol, and MTBE.

3.2.4 Bitter orange characterization

Mature biter oranges fruits were collected at IST Alameda on December 16th of 2020 (harvest of mature oranges), and were dried to constant weight on a vacuum oven and grinded.

3.2.4.1 Bitter orange extractions

Amine extraction [115]: 3.5 g of grinded dried bitter orange was extracted with 10 mL of water for 30 min under magnetic agitation. The samples were then centrifuged and the supernatant was filtered under vacuum. The obtained residue was extracted again using the same procedure and the supernatant was frozen and lyophilised. This was repeated 3 times. The lyophilised samples were redissolved in 20 mL of methanol and analysed in the HPLC.

Flavonoids extraction [115] : 0.4 g of dried bitter orange was extracted with 25 mL of ethanol (80$\%$) for 2 h at 90 ^{o}C under magnetic agitation. The samples was then filtered and the supernatant was concentrated to dryness under vacuum. The solid residue was extracted again using the same procedure for 3 times. The dried samples were redissolved in 12.5 mL of methanol and analysed in the HPLC.

3.2.4.2 Preliminary binding assessment

To test which resin was better for adsorbing synephrine and not the flavonoids, a synthetic mixture of the bitter orange juice was prepared comprising synephrine and naringin as a representative flavonoid. Based on the quantification of these compounds in bitter orange extracts (synephrine and naringin) by Pellati Et al. [115] and on the concentration of these compounds being much lower in the juice than in the peel [70], concentrations of 50 ppm of naringin and 40 ppm of synephrine were mixed in water and the final pH was adjusted to around 2.65 with HCl 4M, as this is the pH reported in the literature for the juice [91].

Binding assays were performed by adding to 2 mL Eppendorf tubes, 25 mg of each resin, and 1 mL of the synthetic bitter orange juice. The Eppendorf tubes were left overnight at room temperature,

under agitation (100 rpm) with magnetic stirring. Each resin was tested in duplicate. After this, the tubes were centrifuged at 10,000 rpm for 3 min, and the supernatant was recovered, lyophilised, redissolved in methanol and analysed by HPLC for synephrine and naringin quantification.

Duplicate samples of the stock solutions (synthetic bitter orange juice) were also analysed by HPLC for synephrine and naringin quantification.

3.2.4.3 Synephrine, naringin and hesperidin quantification and calibration curves

A stock solution of each compound (synephrine, naringin and hesperidin) was prepared by dissolving 25 mg of the pure compounds in 250 mL of methanol (0.1 g/L). The stock solution was then used to obtain solutions of the pure compounds with concentrations between 0.005 g/L and 0.100 g/L (Table 3.4).

A 1.5 mL sample of each solution was then filtered (PTFE syringe filter) and transferred to HPLC vials for HPLC analysis .

Table 3.4: Synephrine, naringin and hesperidin calibration curve dilutions

Concentration (g/L)	Volume from the stock solution (μL)	Final Volume (mL)
0.100	0	250
0.750	7500	10
0.500	2500	10
0.100	1000	10
0.050	500	10
0.020	200	10
0.015	150	10
0.010	100	10
0.005	50	10

For the bitter orange dried extracts HPLC method the calibration curve was then obtained by plotting the area of the peaks at 225 nm of synephrine (Figure A.8), Naringin (Figure A.9) and Hesperidin (Figure A.10) as a function of the concentration .

For the pure compounds on the preliminary Binding assays HPLC method the calibration curve was then obtained by plotting the area of the peak at 225 nm of synephrine (Figure A.11) and the peak at 283 nm of Naringin (Figure A.12), as a function of the concentration.

Chapter 4

Results and Discussion

4.1 Lupin beans Effluent Characterization

Characterising the effluent (Table 4.1) allowed to verify that lupanine is in a higher proportion than other characteristic food ingredients (proteins and sugars). To reach this conclusion, it was necessary to use the Bradford method (Figure A.2) and the DNS method (Figure A.3) to get the total protein and total reducing sugar contents present in the lupin beans effluent. It was possible to determine the presence of 0.13$\pm$0.01 g/L of total Protein and 0.59$\pm$0.01 g/L of total reducing sugars, in the effluent with a lupanine concentration of 3.21$\pm$0.01 g/L.

Concerning lupanine concentration, because of the low linearity of the calibration curve for the concentrations between 0.005 to 2.5 g/L (Figure A.13), the data was split into two concentration intervals comprising low lupanine concentrations (0.005 – 2.5 g/L) and high lupanine concentrations (2.5 – 10 g/L) as presented in Figure A.5 and Figure A.6 respectively.

Table 4.1: Effluent characterisation results

Effluent	Concentration (g/L)
Lupanine	3.21 $\pm$ 0.01
Total Protein	0.13$\pm$ 0.01
Reducing sugars	0.59$\pm$0.01

For the reducing sugar analysis, there was no significant difference verified between the RI chromatograms obtained for the effluent at pH 4 or pH 13 (Figure A.14) being possible to identify in both samples sugars, lactic acid, and citric acid. The basification and subsequent centrifugation of the effluent had no influence on the results. Also, it was not possible to identify the sugars present in the samples due to low resolution of the chromatograms, not allowing to distinguish between glucose and galactose , for example, which were used as reference compounds (figures A.15 and A.16) .

4.2 Bindings for different PBI conditioning

The adsorption of lupanine from the effluent is important not only to further valorise it in the pharmaceutical industry but also by decreasing its concentration in the effluent we can reuse its water for new extractions. We chose PBI as an adsorber because it showed a good performance when it was previously used by our group to adsorb amines and sulfonates [106].

In this report, we evaluated whether the changes made by F. A. Ferreira et al. [106] thermal treatment or different pH conditioning of PBI (pka = 5.5 [104]) polymer could influence the binding of lupanine (pka = 9.1 [101]). The imidazole ring present in the PBI structure can act either as an electron acceptor or as an electron donor and be present in different protonation states depending on the pH. Therefore, the commercial PBI polymer was subject to thermal treatment (PBI-T) to increasing the surface area of the polymer, and also to verify the optimal properties that could improve lupanine adsorption, this PBI-T, was further treated with an acidic (PBI-TA) or basic (PBI-TB) pH conditioning to induce ionic interactions between the polymer and lupanine.

The concentration of lupanine bound to PBI polymers, for this and all the following experiments, was calculated using the lupanine calibration curves described above (Figure A.5 and Figure A.6).

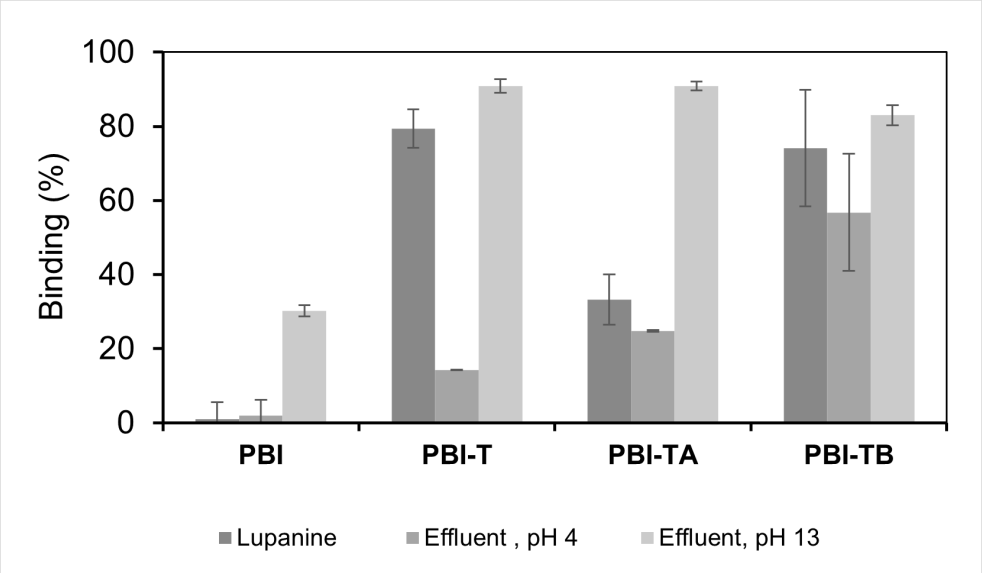

Figure 4.1: Lupanine binding for 100 mg of different PBI polymers in 1 mL of solution at 3 g/L (pure lupanine; effluent at pH 4 or basified with KOH at pH 13) after 17 h of magnetic agitation (100 rpm). PBI: raw material, PBI-T: PBI raw with thermal treatment, PBI-TA: PBI-T with acid treatment, PBI-TB: PBI-T with basic treatment.

From Figure 4.1 it is clear to see that the thermal treatment and pH conditioning improved significantly, the binding of the commercial PBI for lupanine, whether in pure solution or in the effluent. Without basifying the effluent, the higher binding percentage of lupanine was around 50% (for PBI-TB), but higher binding percentages ($> 80\%$) were only obtained after basification of the effluent.

Basified effluent treated with PBI-T had the highest lupanine binding percentage of 91.18 ± 1.69, and if we take a closer look at the results obtained for the basified effluent, the pH conditioning of PBI-T slightly diminished the binding percentage of lupanine, reaching 81.95% for PBI-TA and 83.69% for PBI-TB. If further polymer processing does not improve considerably lupanine binding, it shows to not be feasible to explore these two adsorbers. For this reason, the following experiments only consider the basified effluent and PBI-T.

Lupin beans are biological compounds whose composition changes according to genetic and envi-

ronmental conditions. Because of this, each processed batch results in industrial effluents with differences in chemical and biological composition, leading to variations in lupanine concentration from batch to batch and during storage of the effluent. For example, lupanine concentration in the effluent, after over two months stored at 4 oC, passed from 3.63 g/L to 2.14 g/L. Also, all the different industrial samples collected from and used in this report had lupanine concentrations varying from 4.15 g/L to 2.43 g/L . These changes in effluent composition certainly may not apply only to lupanine but also to all its components (proteins, aminoacids) [58].

This is very important when trying to design a process for lupanine isolation at an industrial scale because we need a robust adsorption protocol able to bind almost all the lupanine from the effluent at different concentrations in different days. From the results obtained, we observed that PBI-T could bind lupanine consistently from all slightly different effluent samples, with lupanine binding with an average around 90 %.

4.2.1 PBI-T efficiency assay

The PBI-T efficiency assay had the aim of testing whether higher volumes of effluent (1 mL; 2 mL; 5 mL; 10 mL; 15 mL; 20 mL; 40 mL) could be treated with the same amount of PBI-T (100 mg) for a given concentration.

From Figure 4.2 we can conclude that increasing the volume, decreased the lupanine binding from 85 % to 3 %.

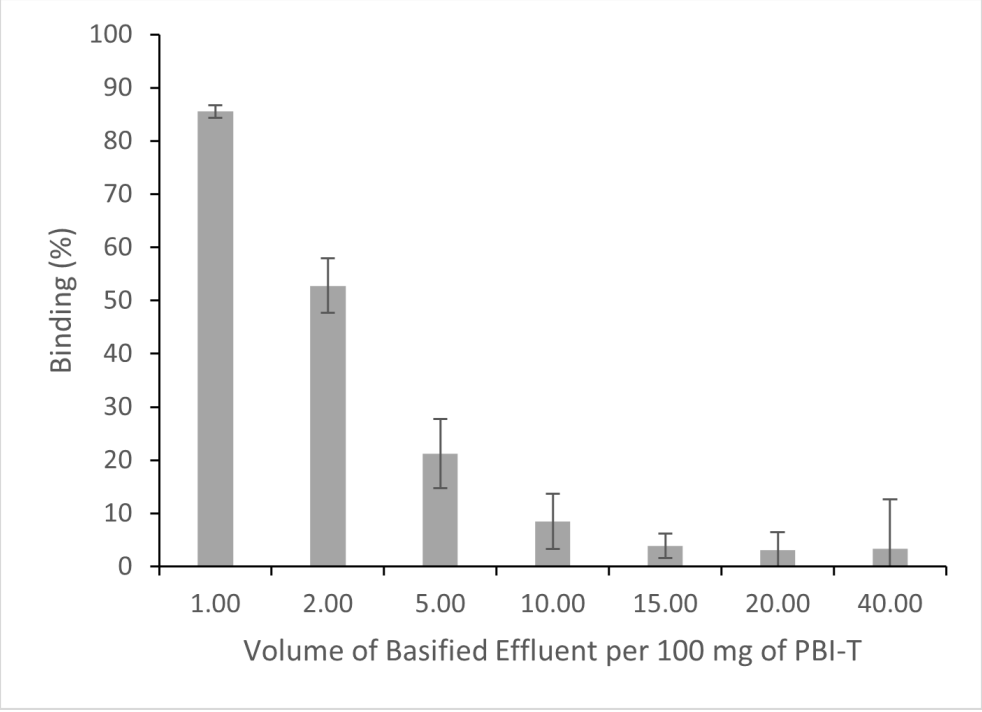

Figure 4.2: Lupanine binding for different volumes of basified effluent at 3 g/L per 100 mg of PBI-T (1 mL; 2 mL; 5 mL; 10 mL ; 15 mL ; 20 mL ; 40 mL) after 17 h of magnetic agitation (100 rpm).

If we look at lupanine binding per concentration of PBI-T in solution, instead of volume (Figure 4.3), it is possible to get a linear relationship, from where we can conclude that to get a binding percentage higher than 80%, PBI-T must be at a concentration close to 100 mg per ml.

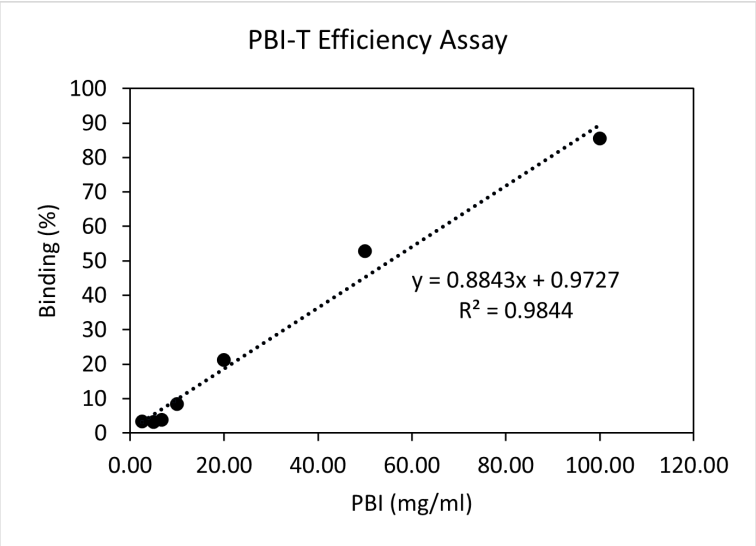

Figure 4.3: Lupanine binding for different concentrations of PBI-T for basified effluent at 3 g/L.

4.2.2 Binding adsorption isotherm experiments

To perform the binding adsorption isotherm experiments, 1 millilitre of basified effluent was added to different amounts of PBI-T, from 10 mg to 100 mg at room temperature and left stirring for 17 h. The concentration of lupanine in each sample was used to determine the amount of lupanine bound to the adsorber PBI-T (q (mg/g)), calculated using equation 3.3, used for the Langmuir (equation 3.4) and Freundlich (equation 3.5) isotherm models.

The experimental data was then plotted according to each model's linearised equations 3.6 and 3.7 (Figure 4.5) and the parameters for each model were calculated (Table 4.2)and used to obtain the theoretical amount of lupanine bound to the adsorber PBI-T (q values) for the experimental concentration of lupanine in solution (C_e) and the results are represented in Figure 4.4.

From the results obtained, it was difficult to say which model fitted better the experimental data, with both models presenting similar R squared values for the linearization. Also, from Figure 4.5 are very similar, with the best fit being the Freundlich model with the highest R squared.

Also, from the Figure 4.4, it is possible to verify that for lupanine concentrations in solution (C_e) below 1500 ppm, both models fit the experimental data, but for higher concentrations, it becomes unclear which model fit's best, so it was necessary to use another common statistical technique used in regression analysis to determine the dispersion of data points, the sum of squares (Equation 4.1).

For a set X of n items:

$$\text{Sum of squares } = \sum_{i=0}^{n} \left(X_i - \bar{X}\right)^2 \tag{4.1}$$

The sum of squares is a measure of deviation from the mean, the distance between each data point and the line of best fit is squared and then summed up. The best fit is the linearisation with the smallest value. By comparing the calculations for the sum of squares for each model (Table 4.2) it is clear that the best fit for our experimental data is the Freundlich model indicating that the adsorber presents a multilayer heterogeneous binding site distribution.

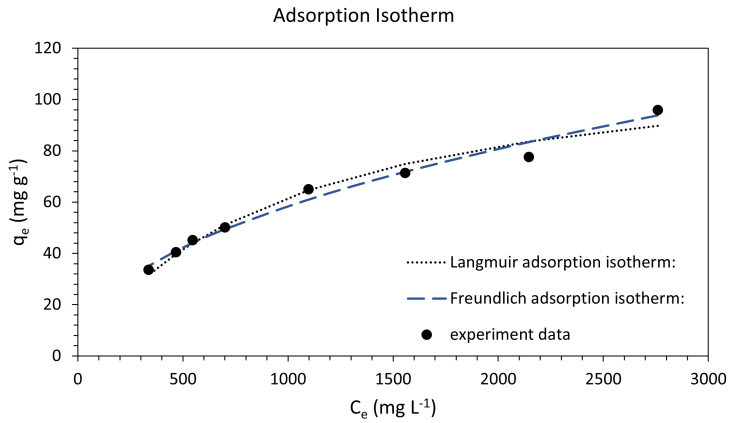

Figure 4.4: Binding adsorption isotherm experiments at room temperature, for 1 mL of basified effluent added to different amounts of PBI-T (10 mg - 100 mg).

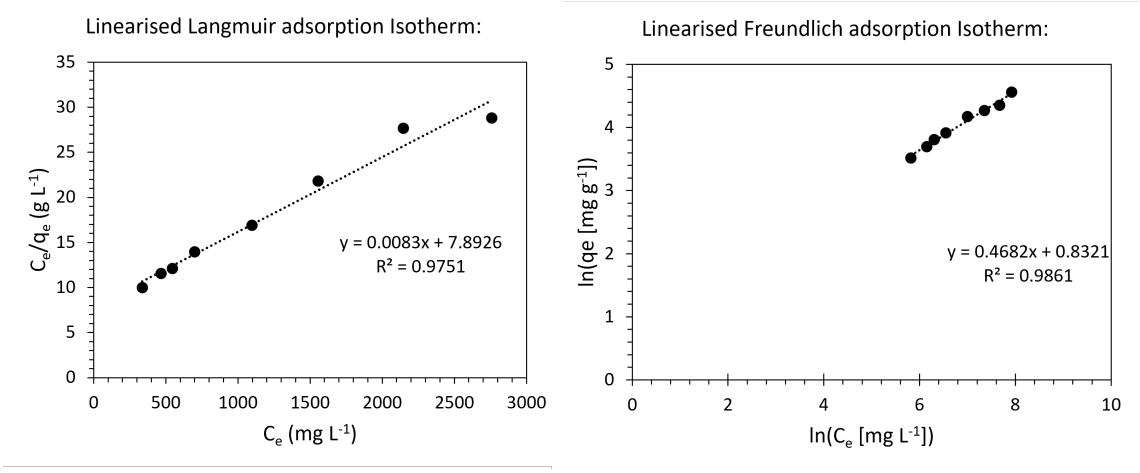

Figure 4.5: Linearization of experimental data for equations of the Langmuir (left) and Freundlich (right) isotherm models.

Table 4.2: Langmuir and Freundlich parameters obtained from the linear trend lines.

Langmuir			**Freundlich**		
Intercept	0.00829	± 0.00054	**Intercept**	0.46818	± 0.02269
Slope	7.89263	± 0.78743	**Slope**	0.83210	± 0.15616
qm (mg/g)	120.69158		**n**	2.13592	
KL (L/mg)	0.00105		**Kf (L/mg)**	2.29813	
Sum of squares	372.33587		**Sum of squares**	0.88664	
R^2	0.97509		**R^2**	0.98610	

4.2.3 Lupanine binding kinetics experiments

To obtain the binding kinetics experiments 1mL of basified effluent was added to 100 mg of PBI-T and left stirring at 100 rpm at room temperature, the reaction was stopped after certain time intervals and lupanine quantified (Figure 4.6), and the adsorption capacity for each time point was calculated from equation 3.3.

The experimental data were fitted to pseudo first- and pseudo-second-order kinetic models using equations 3.8 and 3.9 respectively. From figure 4.7 it is possible to observe that only the pseudo second-order model gave a linear plot representation for the data. The physical parameters determined can be found in Table 4.3 and were used to calculate the theoretical amount of lupanine bound to PBI-T (q_t

values) for each time (t) and the results are represented in Figure 4.6.

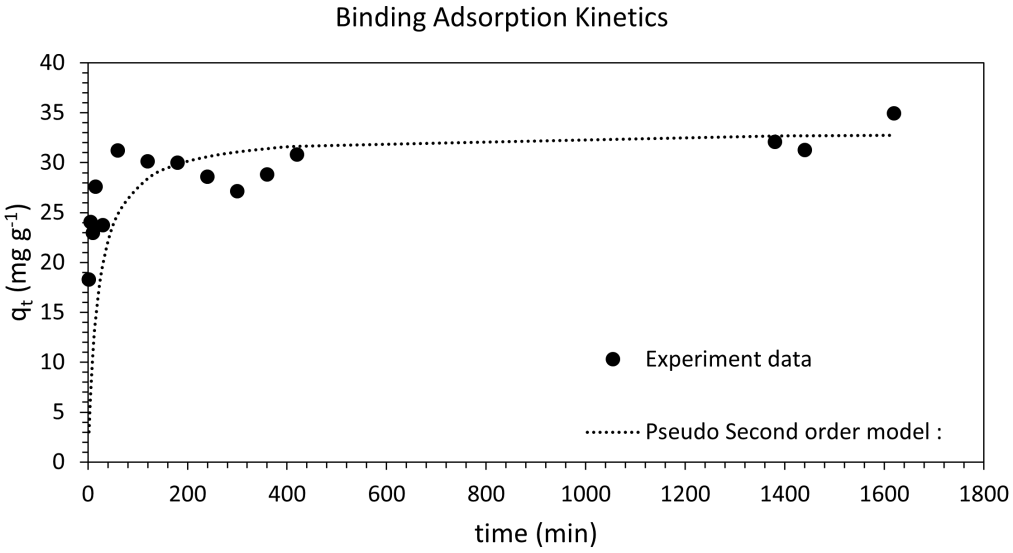

Figure 4.6: Binding kinetics for the basified effluent and PBI-T and theoretical representation of the pseudo-second-order model obtained from the parameters calculated for the experimental data.

Where q_f and q_t (mg/g) are the adsorption capacities at the final and time t (min), respectively.

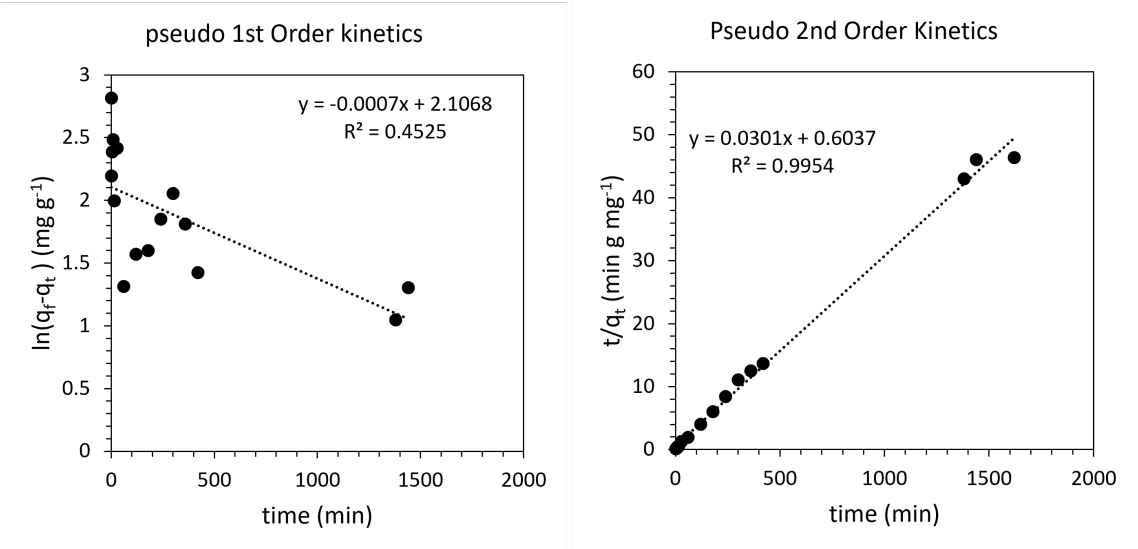

Figure 4.7: Experimental data and equations of the linearised pseudo first- and pseudo-second-order kinetic models' equation 3.8 and 3.9 respectively.

Table 4.3: Parameters obtained for the pseudo-second order kinetics

Pseudo-second order kinetics		
Intercept	0.6037	± 0.3924
Slope	0.0301	± 0.0005
qf (mg/g)	33.171	
K2 (g/ (mg·min)	0.0015	
R^2	0.9954	
Sum of squares	4144.1	

Although we could obtain a good linearization of the data using the pseudo-second-order kinetics model with a good R^2 (Figure 4.7), we could observe some dispersion of the experimental data that was noticeable by the value of the sum of squares (equation 4.1) presented in Table 4.3, this was caused by the lack of experimental data for a long period (overnight) the sum of squares is much lower if we take only in consideration the data obtained in the first 420 minutes (with a value of 290.5).

4.2.4 Binding for different lupanine concentrations

Another binding adsorption assay was performed by changing the concentration of lupanine in solution instead of the amount of PBI-T. This assay was performed by adding to 2 mL Eppendorf tubes, 100 mg of PBI-T, and 1 mL of lupin beans effluent at different lupanine concentrations (previously diluted with water from the concentrated effluent). The tubes were agitated (100 rpm) for 17 h at room temperature with a magnetic stirrer.

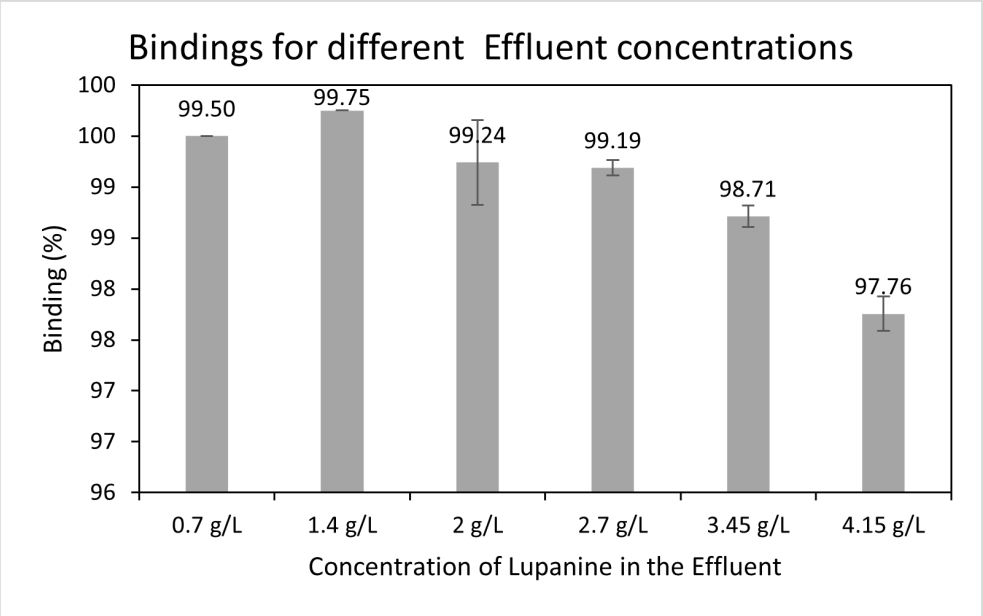

Figure 4.8: Lupanine Binding Percentage for basified effluent with different lupanine concentrations.

Lupanine Binding obtained for the diluted effluent samples with PBI-T were consistent for all the dilutions (99.75-97.76%), showing that the polymer was not saturated. The experimental data were plotted using the linearized equations for the isotherm models (equation 3.6 and equation 3.7) and the parameters obtained are presented on Table 4.4.

Table 4.4: Langmuir and Freundlich parameters obtained from the linear trend line for each isotherm model for different initial lupanine concentrations.

Langmuir			**Freundlich**		
Intercept	0.02021	± 0.00227	**Intercept**	0.486575	± 0.89889
Slope	0.53094	± 0.11121	**Slope**	1.504263	± 0.29579
qm (mg/g)	49.47482		**n**	2.055182	
KL (L/mg)	0.03807		**Kf (L/mg)**	4.500835	
Sum of squares	2.52087		**Sum of squares**	1.841556	
R^2	0.95210		**R^2**	0.879885	

The parameters obtained for the models were used to calculate the theoretical amount of lupanine bound to the adsorber PBI-T (q_t values) for each time (Ce) and the results are represented in Figure

4.9.

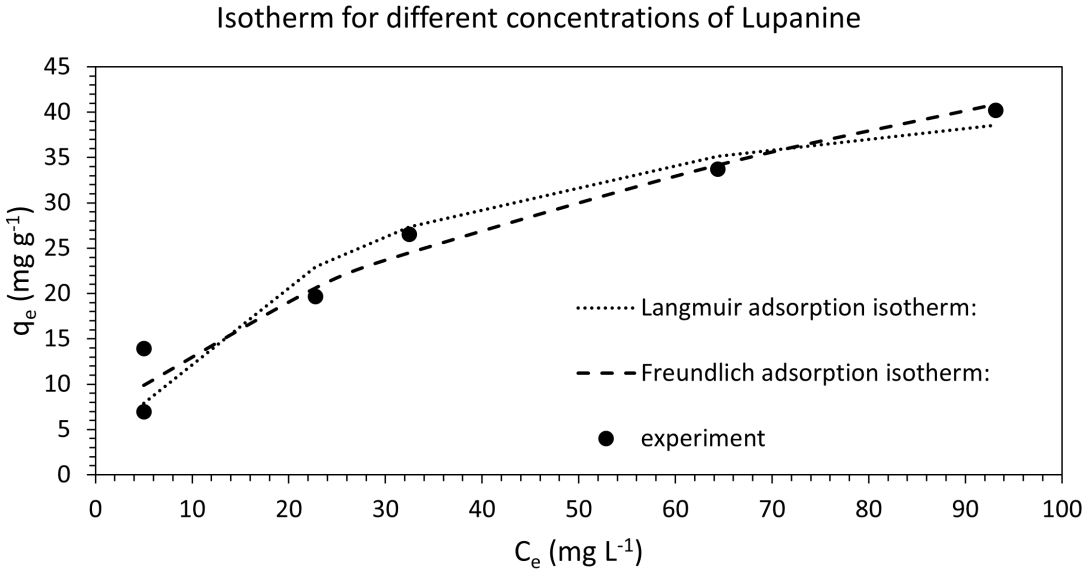

Figure 4.9: Experimental data of PBI-T adsorption capacity obtained for the adsorption assay of the different effluent lupanine concentrations.

The results obtained were so closely related that the theoretical Langmuir and Freundlich models both fit the experimental data. The PBI-T polymer was not saturated so, for a better understanding of this adsorption isotherm, it would be necessary to concentrate the effluent to higher lupanine concentrations, so it could have more experimental data to the model.

4.2.5 Saturation assay

Due to time schedule limitations we were unable to archive higher concentrations of lupanine in the concentrated effluent, so the saturation assays were performed by adding to 2 mL Eppendorf tubes, 100 mg of PBI-T, and 1 mL of basified effluent. The tubes were magnetically stirred (100 rpm) for 17 h at room temperature. After this, the tubes were centrifuged at 10,000 rpm for 3 min, and the supernatant was recovered and analysed for lupanine quantification. The pellet was re-suspended in 1 mL of basified effluent and the process was repeated 3 times.

Table 4.5: Saturation assays for PBI-T

# Binding cycle	**Binding (%)**
1^{st}	89.08 ±1.72
2^{nd}	80.69 ±0.42
3^{rd}	74.52 ±1.73

From the binding kinetics experiment, we observed that after 7 h the adsorption capacity reached a plateau and it was not possible to adsorb higher concentrations of lupanine. However, this saturation experiment shows that, if the effluent is removed after the lupanine binding reached the plateau and a new solution of effluent is added, the adsorber can still bind most of the lupanine from solution (Table 4.5). This could mean that PBI-T could be reused for several binding cycles before performing the recovery of lupanine from the adsorber, diminishing the amount of adsorber necessary to perform the experiments.

4.3 Recovery Assays

In the binding assays, PBI-T presented the highest binding percentages of lupanine, but another important aspect to consider is the recovery of lupanine from the adsorber for further valorisation and also the regeneration of PBI-T. So, the first recovery assays were performed not only for PBI-T but also for PBI-TA and PBI-TB using six different solutions: HCl 0.1M in water, HCL 0.1M in MeOH, DCM, EtOH, THF and EtOAc.

The use of HCl solution aims to explore ionic interactions, the use of alcohols such as MeOH and EtOH (polar protic solvents) aims to break down hydrogen bonds that form during binding and explore the use of weaker interactions (hydrophobic or dipole-dipole), so the combination of MeOH and HCl (HCL 0.1M in MeOH) combine these characteristics. Also, some moderately polar aprotic solvents (DCM, THF and EtOAc) were also chosen to study if they were able to disrupt lupanine/PBI interactions.

After the binding experiment, the solution was centrifuged, the supernatant was used for lupanine quantification and 1mL of a different solvent was added to re-suspended the pellet. The mixture was left at 100 rpm at room temperature for 24 h. After this, the aqueous supernatants were immediately analysed after sample preparations. For the organic solvents, these were collected and evaporated to dryness at room temperature, and the residue was dissolved in water and analysed in HPLC for lupanine quantification. The recovery percentages were calculated using the lupanine concentrations on stock and the concentrations after the binding and recovery with the results being presented in Figure 4.10.

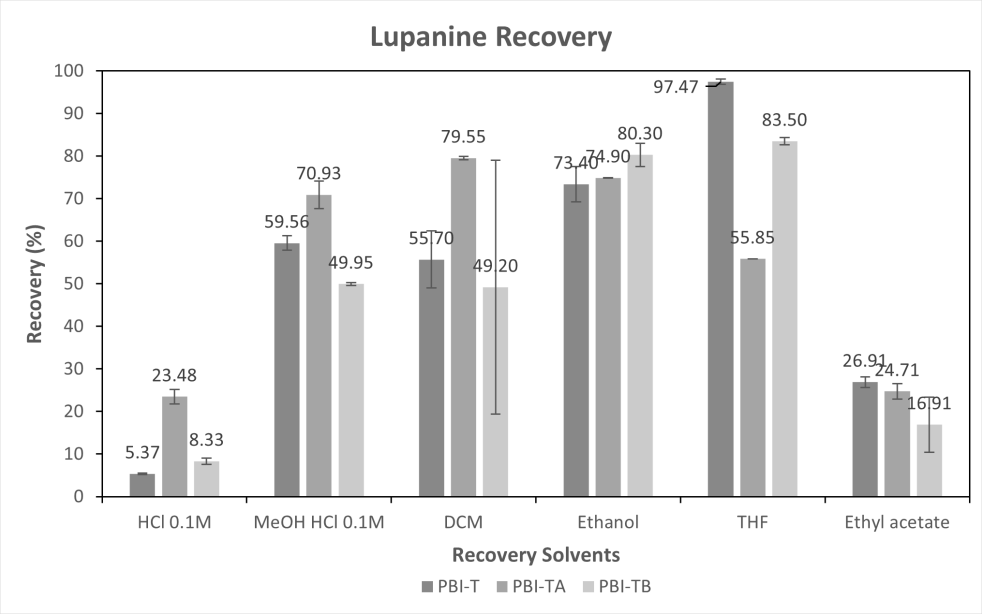

Figure 4.10: Lupanine recovery for the different PBI polymers using several washing solutions. PBI-T: PBI raw polymer with thermal treatment, PBI-TA: PBI-T with acid treatment, PBI-TB: PBI-T with basic treatment.

From Figure 4.10 we observe that the highest recovery for PBI-T was obtained when THF (also the solvent with the highest recovery percentage). For PBI-TB ethanol and THF gave the highest recoveries (around 80 $\%$) and, for PBI-TA it was DCM (79 $\%$).These solvents were able to disrupt the weak interactions between lupanine and PBI releasing lupanine into the medium. However, with DCM, as the polymers used were less dense than DCM they floated and therefore it was difficult to separate the polymer from the solvent through centrifugation, this could present a problem when applying this recovery at the industrial scale .Also, the combination of the HCl interaction with the ionic bonds and the MeOH disruption of hydrogen bonds improved the recovery $\%$ of HCl dissolved in MeOH compared with the

HCl dissolved in water. These results were obtained in a single recovery step.

Considering these results, and the finding that PBI-T showed the best lupanine binding performance, from an economical point of view, the best strategy to isolate lupanine would be to use PBI-T for the binding experiment and THF for the recovery step. Furthermore, for PBI-TA and PBI-TB there is also the need of spending more solvents and time in the processing of the polymer for pH conditioning.

The worst recovery solvents were ethyl acetate and HCl 0.1M in water. With the last one being the only aqueous solution assessed and it had a low concentration of acid. An aqueous solvent based recovery would be the ideal for the recovery step because it would be more environmentally friendly.

So, after these initial results and preliminary findings, other aqueous solutions were tested for PBI-T at room temperature and also at 50^{o}C (Figure 4.11), to test if the slightly higher temperatures influence the solvent diffusion in the porous of the PBI inducing a higher release of lupanine .

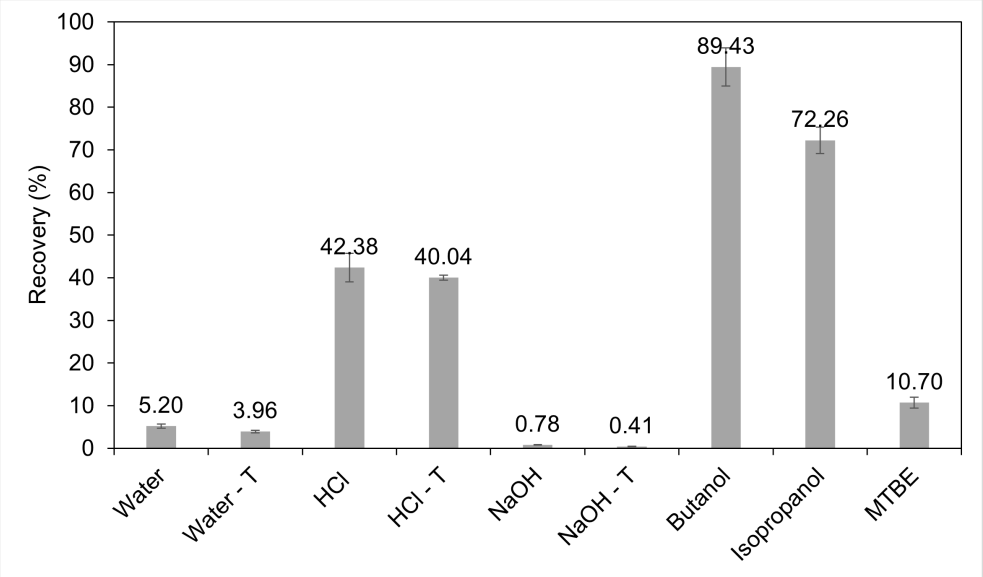

Figure 4.11: Lupanine recovery experiment for PBI-T water at room temperature and at 50 oC (T). HCl: HCl 1M, NaOH: NaOH 1M. Butanol, Isopropanol and MTBE

From the results in Figure 4.11 we can observe that applying temperature did not improve lupanine recovery. Increasing the concentration of HCL from 0.1 M (Figure 4.10) to 1 M (Figure 4.11) increased the recovery from 5.37 $\%$ to 42.38 $\%$. Although not reaching ideal recovery percentages, this result is promising, and in the future, it could be tested in consecutive recovery steps to obtain higher recovery percentages. Although this aqueous solvent may be more environmentally friendly in the end of the recovery we would still have to remove Lupanine from the aqueous medium, which maybe more time consuming and expensive than for an organic solvent.

Since EtOH also presented promising results with 73.40 $\%$ recovery for PBI-T (Figure 4.11), other recovery solvents (butanol, isopropanol and MTBE) were also tested. The results in Figure 4.13 show that butanol and isopropanol could recover more than 70 $\%$ of lupanine, contrary to MTBE that resulted in a low recovery percentage of only around 10 $\%$.

From Figure 4.10 and Figure 4.11, for PBI-T the highest recoveries were obtained for THF (97.47 $\%$) and alcohol solvents, such as ethanol (73.40 $\%$), methanol (59.56 $\%$), butanol (89.43 $\%$) and isopropanol (73.26 $\%$), these alcohols were able to disrupt the weaker interactions and hydrogen bonds that formed during the binding. These results demonstrated that PBI-T could be used to bind and recover Lupanine, without the need to perform a pH conditioning (PBI-TA and PBI-TB) and that several solvents could be chosen to recover lupanine, for higher recovery percentages THF would be the best choice, but a

solvent as ethanol would be more economic and environmentally friendly, although THF has a lower bowling point and it's easier to evaporate decreasing evaporation time (as well as methanol).

We repeated the experiment for the best recovery solvents to assess if the results were reproducible in effluents collect on different days (Figure 4.12).

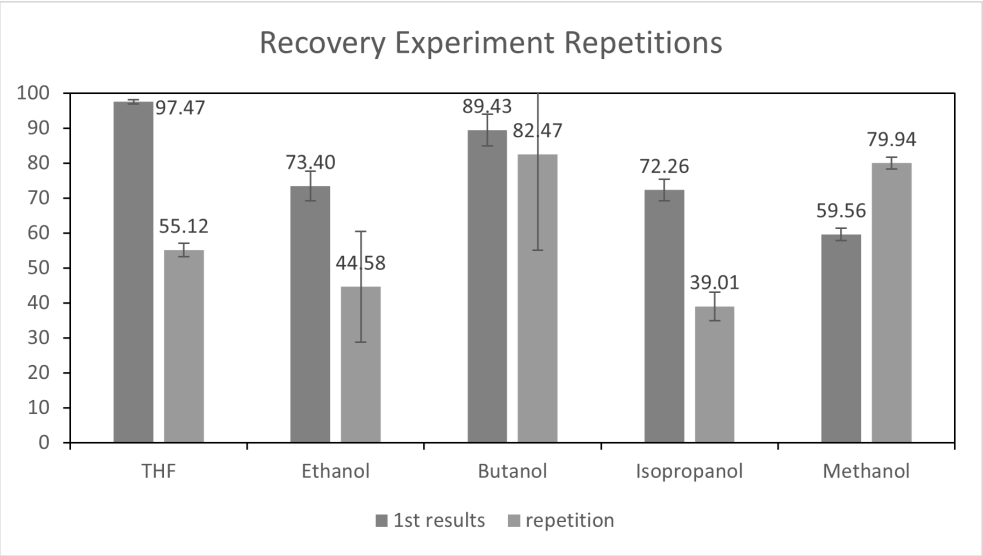

Figure 4.12: Comparison between isolated lupanine Recovery cycles.

As mentioned before the binding results were robust trough out all the experiments, including the repetition results, the average binding for the first results was 91.2 % $\pm$ 1.69 and for the repetition 91.0 $\pm$ 1.96. The results from Figure 4.12 show that the recovery step was not as robust as for the binding experiments. One possible explanation for this decrease in the recovery percentage could be that the composition of the effluent used changed within the time of the first experiments until the repetition was performed, as the lupanine concentration measured in the stock solution had a slight decrease (2.88 g/L of Lupanine for 1st results and 2.55 g/L of Lupanine for the repetition). If the lupanine concentration is different the effluent samples it may also have different concentrations of it's other compounds (such as proteins, sugars and organic acids) that were not quantified in this procedure but may have influenced the recovery, although it did not influence the binding as the binding percentage remained unaltered. Unfortunately, it was not possible to repeat the experiment a third time with a new effluent sample.

4.4 Industrial Case studies

Based on the previous results, SuperPro Designer v10.3 software was used to test the industrial application of lupanine adsorption, from the basified effluent, using PBI-T and butanol for the recovery step, for lupanine isolation. It was assumed an annual factory operating time of 330 days.

Four different case studies were assessed:

1. Effluent 1m^3 - Binding (90%) and best-case recovery (80%) - Gantt Chart on Figure A.17.
2. Effluent 1m^3 - Binding (90%) and worst-case recovery (60%)- Gantt chart on Figure A.17.
3. Effluent 1m^3 - Binding (90%) and two successive worst-case recoveries (60% + 60%) - Gantt chart on Figure A.18.
4. Three successive bindings (90 % + 80 % + 75 %, results based on saturation results of Table 4.5) using the same PBI-T to treat new Effluent (1m^3 effluent added each time) and best-case recovery (80%) - Gantt chart on Figure A.19.

One process scheme was considered for testing the different case studies (Figure 4.13), where it was considered the use of a single reactor for lupanine binding and recovery and a solvent evaporator for the evaporation of butanol after lupanine recovery.

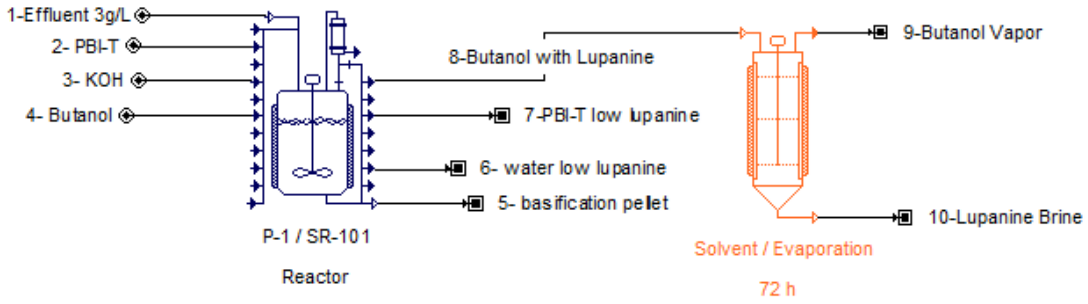

Figure 4.13: Lupanine Industrial Flow sheet Example for the four case studies tested.

Stream one ("1-Effluent 3g/L") on Figure 4.13 corresponds to the effluent with lupanine concentration at 3 g/L from Figure 2.1 on Chapter 2. The overall process data for the different case studies are presented in Table 4.6.

Table 4.6: Overall Process data for the different case studies.

	Case Study 1	Case Study 2	Case Study 3	Case Study 4
Annual Operating Time (days)	328	328	330	328
Lupanine Production Rate (kg/yr)	387	290	261	541
Initial Lupanine Effluent (Kg/batch)	3	3	3	9
Final Lupanine (kg/batch)	2.16	1.62	2.27	5.88
Yield (%)	72	54	76	65
Total Batch Time (h)	45.02	44.6	69.35	86.19
Cycle Time (h)	44.02	44.02	68.77	85.61
Number of Batches per Year	179	179	115	92

The factory operating time are 330 days but as the batch cycles take different amount of hours depending on the procedures, the annual operating time may change, for example for case study 1 and

2 there are 179 batches made per year this corresponds to 328.31 days per year not letting enough time to perform another batch in that year as it takes 45 h to complete a batch.

Case study 1 (best case recovery80 %) as a lupanine production rate of 387 Kg/yr, case study 2 (worst scenario for lupanine recovery - 60 %) decreased the lupanine production rate to 290 Kg/yr. This is a decrease in 25 % of lupanine isolation per year. Also, performing a second recovery step (case study 3), although it increased the lupanine isolated per batch from 1.62 Kg (Case Study 2) to 2.27 kg (Case Study 3), it decreased the annual production rate of lupanine. This happened because the total batch time is 2 times higher, and therefore, fewer batches can be processed per year.

The highest lupanine production rate was achieved for case study 4 (541 Kg of Lupanine per year), although the yield of lupanine (65 %) is lower) than the obtained for the case study 1 (72 %). This can be explained because in case study 4 it is possible to perform the adsorption for 3 consecutive steps without the 24 h intervals required for the lupanine recovery after each binding step. However, this is only feasible for 3 consecutive binding steps (Figure A.19), so, the 92 batches per year of case study 4 can treat more effluent than the 179 batches per year considered for case study 1. So, although less lupanine is recovered from each cubic meter of effluent we can treat more effluent having a higher production rate.

The raw materials needed for the input streams of Figure 4.13 are listed on Table 4.7 and its annual costs on Table 4.8.

Table 4.7: Summary of raw materials needed on the different case studies. Results in Kg of raw material per Kg of lupanine recovered

	Material (Kg/Kg Lupanine)			
Raw material	**Case Study 1**	**Case Study 2**	**Case Study 3**	**Case Study 4**
1-Effluent 3g/L	460.56	614.09	438.63	507.53
2-PBI-T	46.30	61.73	44.1	17.01
3-KOH	8.57	11.42	8.16	9.44
4-Butanol	373.05	497.39	710.56	137.03
TOTAL	888.48	1184.64	1 201.45	671.01

Table 4.8: Summary of annual cost of each raw material needed on the different case studies. Prices of KOH and butanol estimated from Alibaba.com Hong Kong Limited online platform, consulted on October 2021, and PBI-T from PBI Performance Products Inc. (USA)

	Material Annual Cost (€)			
Raw material	**Case Study 1**	**Case Study 2**	**Case Study 3**	**Case Study 4**
PBI-T	4 430 986	4 430 986	2 846 723	2 277 378
KOH	1 003	1 003	645	1 548
Butanol	119 869	119 869	154 022	61 609
TOTAL	4 551 858	4 551 858	3 001 390	2 340 534
Total Cost per g of Lupanine (€)	12	16	11	4

Case study 2 uses the same procedures as case study 1, the only exception is the lower recovery percentage of lupanine after butanol extraction, so it uses the same amount of raw materials per year (Table 4.8)but because it has a lower lupanine yield it needs more raw materials to obtain 1 kg of lupanine. Also, case study 2 is the case study that needs a higher amount of raw materials per kg of lupanine.

Because case study 4 has a lower lupanine yield, it needs a higher amount of effluent to be processed compared with case studies 1 and 3 to obtain 1 kg of lupanine. Since in case study 4, PBI-T is reused, and butanol is only used for every 3 m3 of effluent, this strategy requires PBI-T and less butanol per kg of lupanine than the other case studies, resulting in lower raw material costs.

PBI-T has the highest cost of all the raw materials, corresponding up to 97.34 % of the total annual costs. In case study 4 this cost is decrease by half because it requires less PBI-T per kg of lupanine produced. Another approach that could be studied to decrease even further the costs is reusing PBI-T after lupanine recovery, purging 10 % of the used PBI-T and adding 10 % of new PBI-T after each batch (Figure A.20).

Case study 4 is the one with the best overall results. It has the highest lupanine annual production rate and the lowest annual material cost. Also, it has a total cost of 4.33 €/g of lupanine. Pure lupanine from AOBIOUS INC costs 37.22 €/mg (prices for October 2021) for a minimum purchase of 100 mg giving a price of 37 220 €/g . So, even the highest raw material cost of 16 €/g of lupanine would give a high-profit margin considering that this process would be applied in a small part of the factory that already produces and wastes all this the effluent.

Also, it's estimated a cost of 609 000$ (527 150 €) for the stirred reactor capable of treating 1 m^3 of effluent and 155 000 $ (134 168 €) for the evaporator. Considering the cost of raw materials, labour (single operator 83 €/h), facility dependent costs and laboratory quality control tests, super pro Designer software estimated a total 8 247 000 $ (7 138 603 €) investment needed for implementing Case Study 4. If we sell lupanine at 20 $ per g (17.31 €), the gross margin of case study 4 would be 24 % with a 187 % return of investment and a payback time of 0.54 years (for a 7 % interest) and 10 819 000 $ (9 364 926 €) per year of revenues (Figure A.21).

For the production of 540 Kg of lupanine per year, if it was sold at half the price of the AOBIOUS INC at 21.5$/mg (18,61 €/mg), it would generate a revenue of 11 630 101 314 $ (10 067 015 697 €) per year. Of course there would need to be a buyer that would need these high amounts of lupanine at this price. Also, for these case studies it was assumed that final lupanine was 100 % pure in the brine because there wasn't any experimental data on lupanine purity, so the real profit margin of this project would need to include the price for the purification process of lupanine.

4.5 Bitter Orange Preliminary Study

4.5.1 HPLC detection method

To analyse bitter orange samples, an HPLC method had to be first developed, able to separate its components for further identification and quantification. Hesperidin and naringin are two representative flavonoids present in bitter orange that were available in the lab and were explored for method development. Due to their structural similarities, it was not possible to achieve a good peak separation resorting to a published method by Pellgati Et al. [115] (Figure A.22). So, starting from this point, a new method was developed, and adjusted to our experimental conditions, that allowed the separation and identification of synephrine, naringin and hesperidin. An example of the chromatogram obtained is presented in Figure 4.14.Based on this result, calibration curves were obtained for each compound (Figures A.8 - A.12)

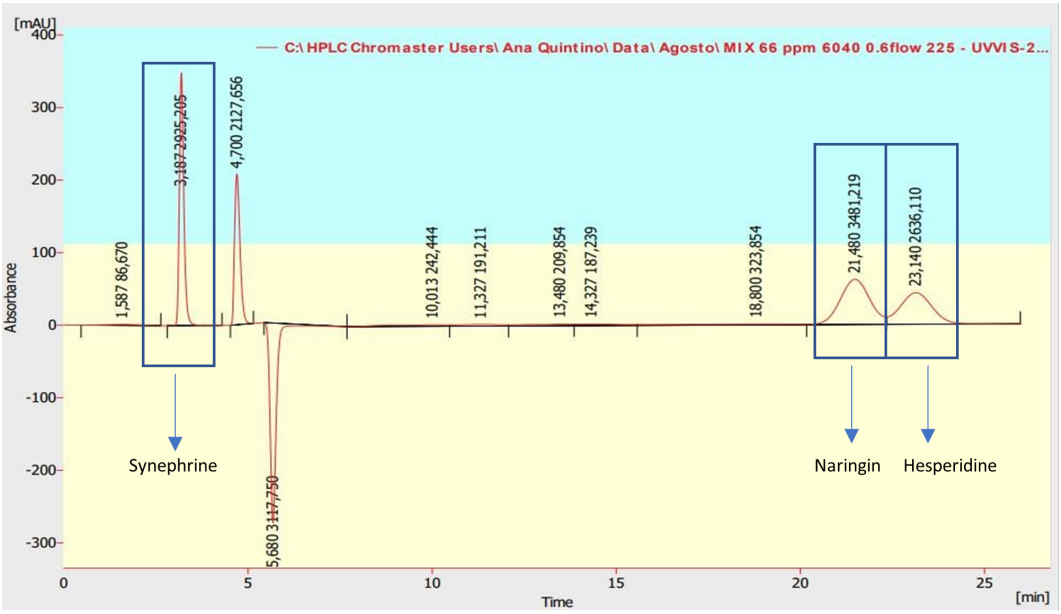

Figure 4.14: Chromatogram obtained for a stock solution containing synephrine, naringin and hesperidin.

4.5.2 Amine extraction

For quantification of synephrine present in bitter oranges collected in IST campus, dried bitter oranges were extracted three times with water, the extract was filtered and lyophilised, and then, it was redissolved in methanol and analysed in the HPLC. Figure 4.15 is an example of the chromatogram obtained for one of these extractions, where the peak of synephrine has a retention time of 3.73 min (this peak was identified using an internal standard) corresponding to a total concentration of 493 ppm, over the 3 extractions (Table 4.9). These results are in accordance with the values obtained in the literature [115].

The calibration curves motioned before were used to quantify synephrine on each extraction (Table 4.9).

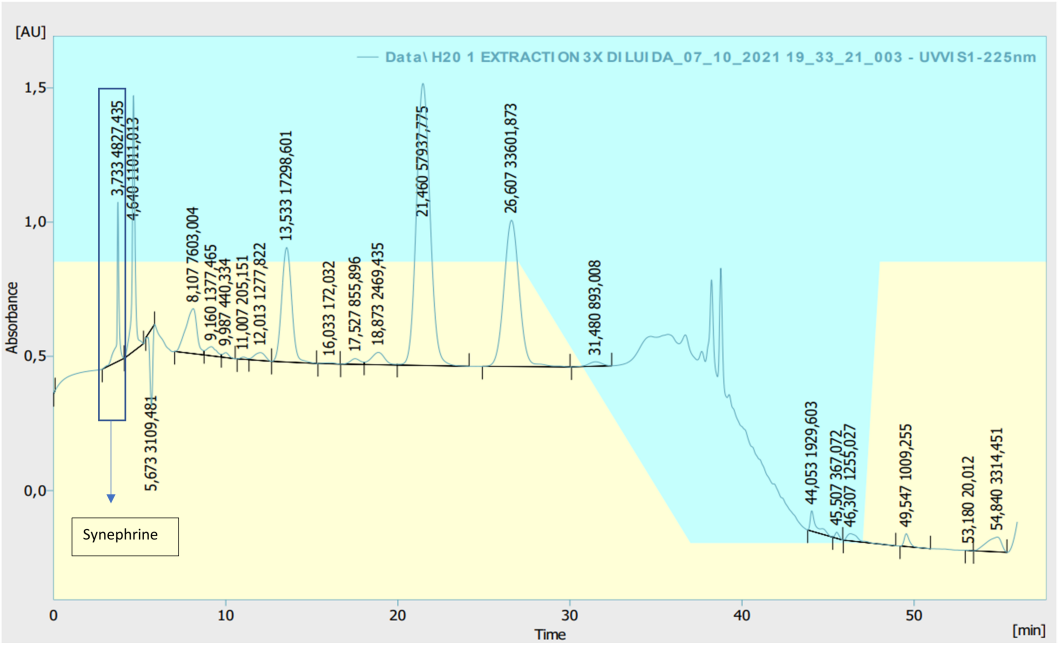

Figure 4.15: Example of chromatogram obtain after the amine extraction 225 nm

Table 4.9: Concentration of synephrine in bitter orange.

# Extraction	Synephrine (ppm)
1	353
2	122
3	18
Total	493

4.5.3 Flavonoids extraction

For flavonoid assessment in bitter oranges collected in IST campus, dried bitter oranges were extracted twice with ethanol. The extracts were filtered and lyophilized, redissolved in methanol and analysed in the HPLC. Figure 4.16 is an example of the chromatogram obtained for one of these extractions, with naringin peak appearing at 21.57 min corresponding to a total concentration of 345 ppm, over the two extractions (Table 4.10). This result are in accordance with the values obtained in the literature [115]. In this sample, hesperidin was not detected .As naringin concentration in bitter orange increases when the fruit matures, and hesperidin diminishes [79], it is natural that we weren't able to detect hesperidin in the extraction samples.

The calibration curves motioned before were used to quantify naringin on each extraction (Table 4.10).

Table 4.10: Concentration of naringin in bitter orange

#Extraction	Naringin (ppm)
1	291
2	54
Total	345

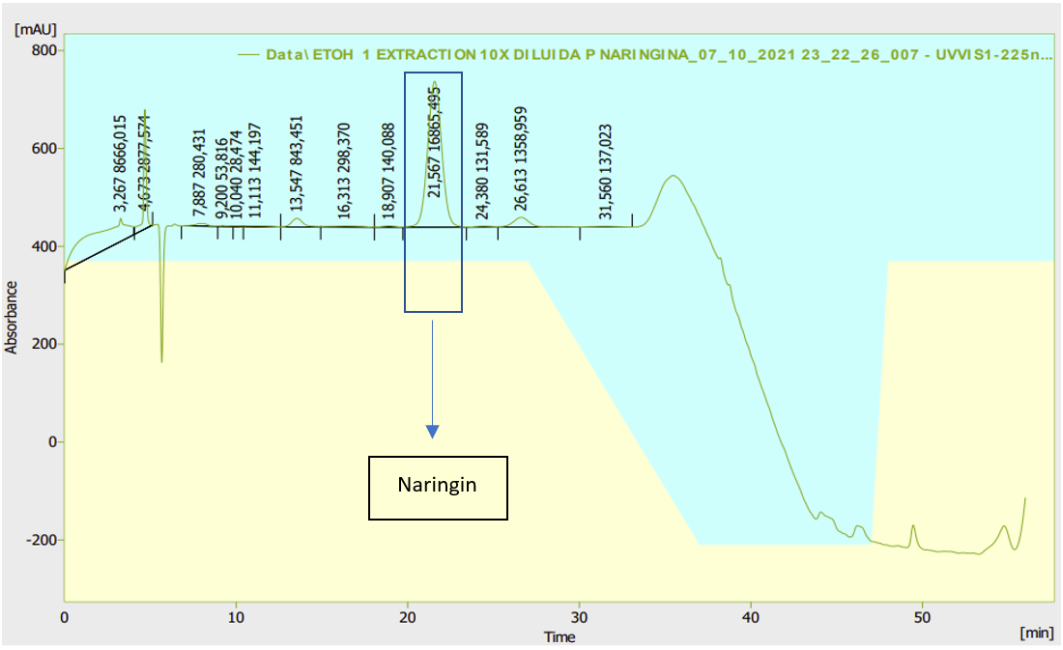

Figure 4.16: Chromatogram obtained after flavonoid extraction from bitter orange.

4.5.4 Synephrine and naringin preliminary binding

Pellati Et. al [115] report synephrine and naringin to be present in mature bitter orange at 500 ppm. There is evidence that the concentration of this compounds are lower in the juice than in the peel [70]. So Based on these values we estimated the concentration of this compounds and prepared a solution at 40 pm and 50 ppm of synephrine and naringin, respectively in water and adjusted the pH of the solution to 2.65 [91], to simulate a synthetic biter orange juice to perform adsorption studies. In these studies, several resins were assessed of different nature.

25 mg of each resin were mixed with 1 mL of the synthetic juice and left overnight at room temperature, under magnetic agitation (100 rpm). Then, the samples were centrifuged and the supernatant was lyophilised and redissolved in methanol for HPLC analysis.

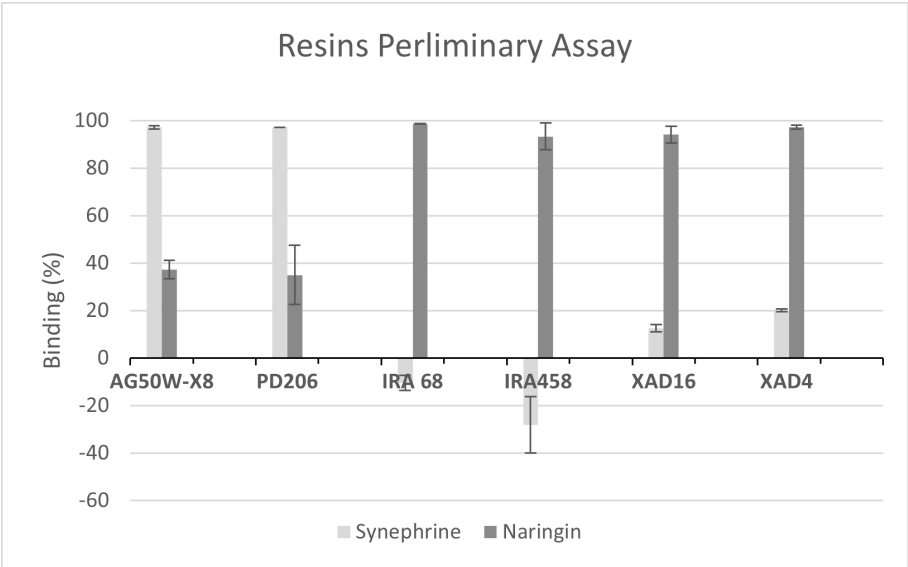

Figure 4.17: Binding Resins perliminary assay

From Figure 4.17 we observe that, for anion exchange resins (IRA-68 and IRA-458) there was some interference in the quantification of synephrine. This can be due to the lack of resin pre-treatment before the binding. For naringin, these resins presented high binding values around 95 $\%$. This same trend was present by the polymeric adsorbent resins (XAD-16 and XAD-4) with naringin binding around 95 $\%$. For these resins, a small amount of synephrine, around 18 $\%$, was also adsorbed. Polymeric adsorbents interact with organic compounds due to the presence of the aromatic rings, as naringin as more aromatic rings than synephrine it had more affinity to these resins. These resins may be useful if we envisage to isolate the flavonoids for further processing, selling or addition to other food formulations for antioxidant properties enhancement, for example.

The cation resins (AG50W-X8 and Purolite PD206) presented the highest bindings for synephrine around 97 $\%$, showing to be ideal adsorbers for synephrine removal from the juice. However, they also adsorbed around 35 $\%$ of naringin. These results are in accordance with the theoretical hypothesis made in the Introduction, where synephrine, having a pKa of 9.76, is protonated in the juice acidic solution, as is present as an ion with a positive charge. Therefore, it was expected that the best resins for the isolation of this compound would be the acid cation exchanger resins.

4.6 Future work

Lupin Beans: Lupanine binding using PBI-T was very successful being able to bind 90 $\%$ of lupanine present in the effluent. It was also possible to recover most of lupanine from the adsorber using butanol as recovery solvent. The next step of this project would be to test cycles of PBI-T binding and lupanine recovery with butanol. It would also be useful to test possible PBI-T regeneration processes for reuse of the adsorber, for example, by repeating the thermal conditioning procedure after a certain number of binding/recovery cycles, when the adsorber starts to lose some of its lupanine binding capacity.

One possible optimisation that would improve this process is to avoid the need to previously basify the effluent, this would help on reusing the water and would be more environmentally friendly. To achieve this, some alterations to PBI conditioning would have to be explored, for example, testing a higher concentration of NaOH on the pH conditioning of PBI-TB, as it was the one who achieved the higher binding percentage for the effluent at pH 4, its usual pH.

Also, the saturation assay performed in this project was left uncompleted due to a malfunction of the HPLC, only being able to complete 3 binding cycles. This experiment could be repeated until PBI-T loses its capacity to bind lupanine and help understand PBI-T maximum adsorption capacity.

To determine the influence of higher lupanine concentrations on PBI-T adsorption process, nanofiltration could be explored to concentrate the effluent, originating a concentrate stream enriched in lupanine and test its influence on PBI-T adsorption, since it was possible to observe in the saturation assay that PBI can still bind more lupanine after a first binding. Repeat the recovery assays, to find a robust solvent that can archive high recovery percentages in different effluent compositions.

The last step, would be to test the scale-up of the procedure to implement on the lupin beans factory.

Bitter Orange: It was impossible to complete all the objectives intended for the bitter orange project in our schedule. For example, the identification of the peaks obtained in the chromatograms for the bitter orange extractions against other flavonoids, and their possible quantification.

Another important step would be analyse bitter orange fresh juice, to compare with the compositions and quantifications reported in the literature and to the extractions of the dried bitter orange. This step would also require testing and, if necessary, adapting the HPLC method to assure a good resolution of the peaks of the compounds present, and also consider a washing step, in the end, to assure that no contaminant may interfere in subsequent runs in the HPLC.

After this step, it would also be possible to perform binding assays for different resins using the fresh juice instead of the synthetic mixture, and ideally find an adsorbent that may bind synephrine or the flavonoids preferentially in the orange juice. If that is not possible, then another alternative may the use of molecularly imprinted polymers (MIP) to bind specifically one of the species, these are able to mimic natural recognition entities, such as antibodies and biological receptors or in our case amines, and are very useful to separate and analyse complicated samples.

Also, it would be necessary to test recovery solvents and regeneration steps for the resins with the highest binding percentages of each type of compounds.

Finally, it would be useful to do a scale-up of the laboratory process to be applied in the food industry.

Chapter 5

Conclusion

Lupanine is present in the effluent at a concentration of 3 g/L, the effluent also contains sugars, proteins, lactic and citric acid. The thermal treatment and pH conditionings used on commercial PBI improved the binding percentage of Lupanine. PBI-T had the highest binding percentage for Lupanine pure solution and the basified effluent. PBI-TB had the highest binding percentage for the pure effluent.

When trying to reduce the amount of PBI needed to treat the industrial effluent, increasing the volume of effluent while maintaining the amount of PBI-T it decreased the binding percentage of Lupanine. It was possible to get a linear relationship between the amount of PBI per ml of Effluent and the binding percentage, proving that we could not reduce the amount of PBI needed to treat the effluent. The saturation assay help to understand how to reduce the amount of PBI needed because the same PBI could bind more volume of lupanine if the treated effluent was removed and new untreated effluent added to the same PBI, the second binding had a binding percentage of 80.69 $\% \pm 0.42$.

The binding kinetics showed that PBI-T binding follows the pseudo-second-order kinetics with a maximum adsorption capacity of 33 mg of Lupanine per g of PBI-T this value corresponds to the amount of lupanine present in the 1ml effluent added to PBI-T, so in the future, it should be tested if this value of maximum adsorption capacity is the same for higher concentrations of lupanine in the effluent. The Binding Adsorption Isotherm for PBI-T showed that PBI-T follows the Freundlich adsorption model(n = 2.14 and K_f = 2.30).

The first preliminary recovery assay showed that using PBI-T and THF was the best method for lupanine binding and recovery. But further testing on different effluents from different days collected from the same factory and industrial process showed that PBI-T was always effective in binding lupanine from every effluent (average binding percentage of 90 $\%$) and that the recovery results were not reproducible.

The extractions of dried bitter Oranges with water (amine extraction) and ethanol (flavonoids extraction) got a concentration of 493 ppm of synephrine and 345 ppm of naringin, there wasn't detected any amount of hesperidin. A preliminary binding assay was performed with a synthetic mixture of bitter orange juice (40 ppm of synephrine; 50 ppm naringin pH 2.65) mixed with 25 mg of resin (2 acidic resins, 2 basic resins and 2 polymeric adsorbers), from which the acidic resins were the best to bind synephrine while keeping most of the healthy flavonoid (naringin) in solution.

Ideally, after some more optimizations and scale-up tests, it will be possible to remove these alkaloids from their food products and get a source of healthy food products that came from agricultural plantations that are resistant to drought and climate alterations that could help produce food in harsh conditions.

Bibliography

[1] A. Garrido, M. R. Llamas, C. Varela-Ortega, P. Novo, R. Rodríguez-Casado, and M. M. Aldaya, *Water footprint and virtual water trade in Spain: Policy implications*, vol. 35. Springer Science & Business Media, 2010.

[2] M. Li, Y. Xu, Q. Fu, V. P. Singh, D. Liu, and T. Li, "Efficient irrigation water allocation and its impact on agricultural sustainability and water scarcity under uncertainty," *Journal of Hydrology*, p. 124888, 2020.

[3] A. Nardone, B. Ronchi, N. Lacetera, M. S. Ranieri, and U. Bernabucci, "Effects of climate changes on animal production and sustainability of livestock systems," *Livestock Science*, vol. 130, no. 1-3, pp. 57–69, 2010.

[4] P. Annicchiarico, M. Romani, and L. Pecetti, "White lupin (lupinus albus) variation for adaptation to severe drought stress," *Plant Breeding*, vol. 137, no. 5, pp. 782–789, 2018.

[5] P. Shirgure, L. Ram, S. Singh, R. Marathe, and R. Yadav, "Water-use and growth of acid lime (citrus aurantifolia) under different irrigation systems," *Indian Journal of Agricultural Sciences*, vol. 70, pp. 125–127, 02 2000.

[6] A. J. Huxley, M. Griffiths, *et al.*, *Dictionary of gardening*. Stockton Press, 1992.

[7] S. Clark, "Plant guide for white lupine (lupinus albus l.)," *USDA-Natural Resources Conservation Service, Big Flats Plant Materials Center. Corning, New York*, 2014.

[8] B. S. Kurlovich, *Lupins: geography, classification, genetic resources and breeding*. Bogouslav Kourlovitch, 2002.

[9] J. Pothier, S.-L. CHEAV, N. Galand, C. Dormeau, and C. Viel, "A comparative study of the effects of sparteine, lupanine and lupin extract on the central nervous system of the mouse," *Journal of pharmacy and pharmacology*, vol. 50, no. 8, pp. 949–954, 1998.

[10] M. Erbaş, M. Certel, and M. Uslu, "Some chemical properties of white lupin seeds (lupinus albus l.)," *Food Chemistry*, vol. 89, no. 3, pp. 341 – 345, 2005.

[11] M. Wink, C. Meißner, and L. Witte, "Patterns of quinolizidine alkaloids in 56 species of the genus lupinus," *Phytochemistry*, vol. 38, no. 1, pp. 139–153, 1995.

[12] M. Erbaş, M. Certel, and M. Uslu, "Some chemical properties of white lupin seeds (lupinus albus l.)," *Food chemistry*, vol. 89, no. 3, pp. 341–345, 2005.

[13] I. J. Karoui, W. A. Wannes, and B. Marzouk, "Refined corn oil aromatization by citrus aurantium peel essential oil," *Industrial Crops and Products*, vol. 32, no. 3, pp. 202–207, 2010.

[14] H. Nguyen, E. M. Campi, W. R. Jackson, and A. F. Patti, “Effect of oxidative deterioration on flavour and aroma components of lemon oil,” *Food Chemistry*, vol. 112, no. 2, pp. 388–393, 2009.

[15] I. Suntar, H. Khan, S. Patel, R. Celano, and L. Rastrelli, “An overview on citrus aurantium l.: its functions as food ingredient and therapeutic agent,” *Oxidative medicine and cellular longevity*, vol. 2018, 2018.

[16] S. Carmali, V. D. Alves, I. M. Coelhoso, L. M. Ferreira, and A. M. Lourenço, “Recovery of lupanine from lupinus albus l. leaching waters,” *Separation and purification technology*, vol. 74, no. 1, pp. 38–43, 2010.

[17] U. DESA, “United nations department of economic and social affairs/population division (2009b): World population prospects: The 2008 revision,” *Internet: http://esa. un. org/unpp (gelesen am 16*, 2010.

[18] M. A. Cole and E. Neumayer, “Examining the impact of demographic factors on air pollution,” *Population and Environment*, vol. 26, no. 1, pp. 5–21, 2004.

[19] R. I. McDonald, P. Green, D. Balk, B. M. Fekete, C. Revenga, M. Todd, and M. Montgomery, “Urban growth, climate change, and freshwater availability,” *Proceedings of the National Academy of Sciences*, vol. 108, no. 15, pp. 6312–6317, 2011.

[20] V. Masson-Delmotte, A. Zhai, S. Pirani, C. Connors, S. Péan, N. Berger, Y. Caud, L. Chen, I. Goldfarb, M. Gomis, K. Huang, E. Leitzell, J. Lonnoy, T. Matthews, T. Maycock, O. Waterfield, R. Yelekçi, Yu, and Zhou, “Ipcc, 2021: Climate change 2021: The physical science basis. contribution of working group i to the sixth assessment report of the intergovernmental panel on climate change,” vol. Cambridge University Press. In Press., 2021.

[21] M. Barrett, A. Belward, S. Bladen, T. Breeze, N. Burgess, S. Butchart, H. Clewclow, S. Cornell, A. Cottam, S. Croft, *et al.*, “Living planet report 2018: Aiming higher,” 2018.

[22] R. Chambers, “Knowledge systems for inclusively responsible food and agriculture,” in *Rethinking Food and Agriculture*, pp. 353–369, Elsevier, 2020.

[23] E. K. G. Umwelt and E. C. E. Directorate-General, *The Factory of Life: Why Soil Biodiversity is So Important*. Office for Official Publications of the European Union, 2010.

[24] C. Wagg, S. F. Bender, F. Widmer, and M. G. van der Heijden, “Soil biodiversity and soil community composition determine ecosystem multifunctionality,” *Proceedings of the National Academy of Sciences*, vol. 111, no. 14, pp. 5266–5270, 2014.

[25] M. A. Tsiafouli, E. Thébault, S. P. Sgardelis, P. C. De Ruiter, W. H. Van Der Putten, K. Birkhofer, L. Hemerik, F. T. De Vries, R. D. Bardgett, M. V. Brady, *et al.*, “Intensive agriculture reduces soil biodiversity across europe,” *Global change biology*, vol. 21, no. 2, pp. 973–985, 2015.

[26] R. Yin, P. Kardol, M. P. Thakur, I. Gruss, G.-L. Wu, N. Eisenhauer, and M. Schädler, “Soil functional biodiversity and biological quality under threat: Intensive land use outweighs climate change,” *Soil Biology and Biochemistry*, p. 107847, 2020.

[27] G. T. Cushman, “David r. montgomery. dirt: The erosion of civilizations. ix+ 285 pp., illus., bibl., index. berkeley: University of california press, 2007. $24.95,” 2008.

[28] E. González-Sánchez and G. Basch, “Conservation agriculture: Making climate change mitigation and adaptation real in europe,” 2017.

[29] E. Ojea, S. E. Lester, and D. Salgueiro-Otero, “Adaptation of fishing communities to climate-driven shifts in target species,” *One Earth*, 2020.

[30] A. Mood and P. Brooke, “Estimating the number of farmed fish killed in global aquaculture each year,” *Fishcount. org. uk*, vol. 1, 2012.

[31] B. Worm, E. B. Barbier, N. Beaumont, J. E. Duffy, C. Folke, B. S. Halpern, J. B. Jackson, H. K. Lotze, F. Micheli, S. R. Palumbi, *et al.*, “Impacts of biodiversity loss on ocean ecosystem services,” *science*, vol. 314, no. 5800, pp. 787–790, 2006.

[32] J. A. Foley, N. Ramankutty, K. A. Brauman, E. S. Cassidy, J. S. Gerber, M. Johnston, N. D. Mueller, C. O’Connell, D. K. Ray, P. C. West, *et al.*, “Solutions for a cultivated planet,” *Nature*, vol. 478, no. 7369, pp. 337–342, 2011.

[33] H. Steinfeld, P. Gerber, T. Wassenaar, V. Castel, M. Rosales, M. Rosales, and C. de Haan, *Livestock’s long shadow: environmental issues and options*. Food & Agriculture Org., 2006.

[34] F. R. Rijsberman, “Water scarcity: fact or fiction?,” *Agricultural water management*, vol. 80, no. 1-3, pp. 5–22, 2006.

[35] R. Bailey, A. Froggatt, and L. Wellesley, “Livestock–climate change’s forgotten sector,” *Chatham House*, 2014.

[36] D. Tilman, J. Fargione, B. Wolff, C. D’Antonio, A. Dobson, R. Howarth, D. Schindler, W. H. Schlesinger, D. Simberloff, and D. Swackhamer, “Forecasting agriculturally driven global environmental change,” *science*, vol. 292, no. 5515, pp. 281–284, 2001.

[37] S. FOOD, “Global initiative on food loss and waste reduction,” *Key facts on food loss and waste you should know*, pp. 1–2, 2015.

[38] W. H. Organization *et al.*, “Noncommunicable diseases country profiles 2018,” 2018.

[39] Unicef, W. H. Organization, *et al.*, *The state of food security and nutrition in the world 2017: Building resilience for peace and food security*. Food and Agriculture Organization of the United Nations, 2017.

[40] H. N. Lazarides, “Hunger and obesity: Is this the best we–food scientists/engineers-can offer to the world community in the 21st century?,” *Procedia Food Science*, vol. 1, pp. 1854–1860, 2011.

[41] W. H. Organization, *Diet, nutrition, and the prevention of chronic diseases: report of a joint WHO/FAO expert consultation*, vol. 916. World Health Organization, 2003.

[42] P. Poirier and R. H. Eckel, “Obesity and cardiovascular disease,” *Current atherosclerosis reports*, vol. 4, no. 6, pp. 448–453, 2002.

[43] L.-J. Zhao, Y.-J. Liu, P.-Y. Liu, J. Hamilton, R. R. Recker, and H.-W. Deng, “Relationship of obesity with osteoporosis,” *The Journal of Clinical Endocrinology & Metabolism*, vol. 92, no. 5, pp. 1640–1646, 2007.

[44] S. Brebaum and G. Boland, “Sweet white lupin: A potential crop for ontario,” *Canadian Journal of Plant Science*, vol. 75, no. 4, pp. 841–849, 1995.

[45] M. Muzquiz, C. Cuadrado, G. Ayet, C. de la Cuadra, C. Burbano, and A. Osagie, “Variation of alkaloid components of lupin seeds in 49 genotypes of lupinus albus from different countries and locations.,” *Journal of Agricultural and Food Chemistry*, vol. 42, no. 7, pp. 1447–1450, 1994.

[46] C. Di Lorenzo, A. Dos Santos, F. Colombo, E. Moro, M. Dell'Agli, and P. Restani, "Development and validation of hplc method to measure active amines in plant food supplements containing citrus aurantium l," *Food Control*, vol. 46, pp. 136 – 142, 2014.

[47] K. M. Frick, L. G. Kamphuis, K. H. Siddique, K. B. Singh, and R. C. Foley, "Quinolizidine alkaloid biosynthesis in lupins and prospects for grain quality improvement," *Frontiers in Plant Science*, vol. 8, p. 87, 2017.

[48] F. Pellati, S. Benvenuti, and M. Melegari, "Enantioselective lc analysis of synephrine in natural products on a protein-based chiral stationary phase," *Journal of pharmaceutical and biomedical analysis*, vol. 37, no. 5, pp. 839–849, 2005.

[49] M. Mousavi-Derazmahalleh, B. Nevado, P. E. Bayer, D. A. Filatov, J. K. Hane, D. Edwards, W. Erskine, and M. N. Nelson, "The western mediterranean region provided the founder population of domesticated narrow-leafed lupin," *Theoretical and Applied Genetics*, vol. 131, no. 12, pp. 2543–2554, 2018.

[50] B. Dinkelaker, V. Römheld, and H. Marschner, "Citric acid excretion and precipitation of calcium citrate in the rhizosphere of white lupin (lupinus albus l.)," *Plant, Cell & Environment*, vol. 12, no. 3, pp. 285–292, 1989.

[51] C. Pinheiro, J. A. Passarinho, and C. P. Ricardo, "Effect of drought and rewatering on the metabolism of lupinus albus organs," *Journal of Plant Physiology*, vol. 161, no. 11, pp. 1203 – 1210, 2004.

[52] M. M. Lucas, F. L. Stoddard, P. Annicchiarico, J. Frias, C. Martinez-Villaluenga, D. Sussmann, M. Duranti, A. Seger, P. M. Zander, and J. J. Pueyo, "The future of lupin as a protein crop in europe," *Frontiers in plant science*, vol. 6, p. 705, 2015.

[53] J.-C. Favier, J. Ireland-Ripert, C. Toque, and M. Feinberg, *Répertoire général des aliments: table de composition= composition tables*. 1995.

[54] C. Huyghe, "White lupin (lupinus albus l.)," *Field Crops Research*, vol. 53, no. 1-3, pp. 147–160, 1997.

[55] D. Resta, G. Boschin, A. D'Agostina, and A. Arnoldi, "Evaluation of total quinolizidine alkaloids content in lupin flours, lupin-based ingredients, and foods," *Molecular nutrition & food research*, vol. 52, no. 4, pp. 490–495, 2008.

[56] S. Tyski, M. Markiewicz, K. Gulewicz, and T. Twardowski, "The effect of lupin alkaloids and ethanol extracts from seeds of lupinus angustifolius on selected bacterial strains," *Journal of plant physiology*, vol. 133, no. 2, pp. 240–242, 1988.

[57] F. Zamora-Natera, P. García-López, M. Ruiz-López, and E. Salcedo-Pérez, "Composición de alcaloides en semillas de lupinus mexicanus (fabaceae) y evaluación antifúngica y alelopática del extracto alcaloideo," *Agrociencia*, vol. 42, no. 2, pp. 185–192, 2008.

[58] C. B. M. Barbeitos, *Towards the development of a process for lupin beans detoxification wastewater with lupanine recovery.* Master thesis in Biological Engineering, Instituto Superior Técnico, Universidade de Lisboa., 2016.

[59] W. Cowling, C. Huyghe, and W. Swiecicki, "Lupin breeding," 1998.

[60] M. Kroc, W. Rybiński, P. Wilczura, K. Kamel, Z. Kaczmarek, P. Barzyk, and W. Święcicki, "Quantitative and qualitative analysis of alkaloids composition in the seeds of a white lupin (lupinus albus l.) collection," *Genetic Resources and Crop Evolution*, vol. 64, no. 8, pp. 1853–1860, 2017.

[61] F. C. Santana and J. Empis, "Bacterial removal of quinolizidine alkaloids from lupinus albus flours," *European Food Research and Technology*, vol. 212, no. 2, pp. 217–224, 2001.

[62] T. Esteves, A. T. Mota, C. Barbeitos, K. Andrade, C. A. Afonso, and F. C. Ferreira, "A study on lupin beans process wastewater nanofiltration treatment and lupanine recovery," *Journal of Cleaner Production*, vol. 277, p. 123349, 2020.

[63] C. R. Sirtori, M. R. Lovati, C. Manzoni, S. Castiglioni, M. Duranti, C. Magni, S. Morandi, A. D'Agostina, and A. Arnoldi, "Proteins of white lupin seed, a naturally isoflavone-poor legume, reduce cholesterolemia in rats and increase ldl receptor activity in hepg2 cells," *The Journal of nutrition*, vol. 134, no. 1, pp. 18–23, 2004.

[64] J. M. Martins, M. Riottot, M. C. de Abreu, A. M. Viegas-Crespo, M. J. Lança, J. A. Almeida, J. B. Freire, and O. P. Bento, "Cholesterol-lowering effects of dietary blue lupin (lupinus angustifolius l.) in intact and ileorectal anastomosed pigs," *Journal of Lipid Research*, vol. 46, no. 7, pp. 1539–1547, 2005.

[65] M. del Carmen Millán-Linares, B. Bermúdez, M. del Mar Yust, F. Millán, and J. Pedroche, "Anti-inflammatory activity of lupine (lupinus angustifolius l.) protein hydrolysates in thp-1-derived macrophages," *Journal of Functional Foods*, vol. 8, pp. 224 – 233, 2014.

[66] L. P. García, P. G. de la Mora, W. Wysocka, B. Maiztegui, M. E. Alzugaray, H. Del Zotto, and M. I. Borelli, "Quinolizidine alkaloids isolated from lupinus species enhance insulin secretion.," *European journal of Pharmacology*, vol. 504, no. 1-2, p. 139, 2004.

[67] S. Parmaki, I. Vyrides, M. I. Vasquez, V. Hartman, I. Zacharia, I. Hadjiadamou, C. B. Barbeitos, F. C. Ferreira, C. A. Afonso, C. Drouza, and M. Koutinas, "Bioconversion of alkaloids to high-value chemicals: Comparative analysis of newly isolated lupanine degrading strains," *Chemosphere*, vol. 193, pp. 50 – 59, 2018.

[68] D. De Santis and M. T. Frangipane, "Citrus aurantium l.: Cultivar impact on sensory profile," *International Journal of Gastronomy and Food Science*, vol. 20, p. 100203, 2020.

[69] C. Zhang, P. Bucheli, X. Liang, and Y. Lu, "Citrus flavonoids as functional ingredients and their role in traditional chinese medicine," *Food*, vol. 1, pp. 287–296, 2007.

[70] S. Ersus and M. Cam, "Determination of organic acids, total phenolic content, and antioxidant capacity of sour citrus aurantium fruits," *Chemistry of Natural Compounds*, vol. 43, no. 5, p. 607–609, 2007.

[71] R. Phillips and M. Rix, *Conservatory and Indoor Plants: Plants for Warm Gardens*, vol. 2. Pan Macmillan, 1998.

[72] W. Bank, "Average precipitation in depth (mm per year)," 2015.

[73] M. Zielińska-Przyjemska and E. Ignatowicz, "Citrus fruit flavonoids influence on neutrophil apoptosis and oxidative metabolism," *Phytotherapy Research: An International Journal Devoted to Pharmacological and Toxicological Evaluation of Natural Product Derivatives*, vol. 22, no. 12, pp. 1557–1562, 2008.

[74] K. Itoh, M. Masuda, S. Naruto, K. Murata, and H. Matsuda, "Antiallergic activity of unripe citrus hassaku fruits extract and its flavanone glycosides on chemical substance-induced dermatitis in mice," *Journal of natural medicines*, vol. 63, no. 4, pp. 443–450, 2009.

[75] O. Benavente-Garcia and J. Castillo, "Update on uses and properties of citrus flavonoids: new findings in anticancer, cardiovascular, and anti-inflammatory activity," *Journal of agricultural and food chemistry*, vol. 56, no. 15, pp. 6185–6205, 2008.

[76] C. A. da Camara, Y. Akhtar, M. B. Isman, R. C. Seffrin, and F. S. Born, "Repellent activity of essential oils from two species of citrus against tetranychus urticae in the laboratory and greenhouse," *Crop Protection*, vol. 74, pp. 110–115, 2015.

[77] K.-I. Park, H.-S. Park, M.-K. Kim, G.-E. Hong, A. Nagappan, H.-J. Lee, S. Yumnam, W.-S. Lee, C.-K. Won, S.-C. Shin, and G.-S. Kim, "Flavonoids identified from korean citrus aurantium l. inhibit non-small cell lung cancer growth in vivo and in vitro," *Journal of Functional Foods*, vol. 7, pp. 287 – 297, 2014.

[78] M. K. Anwer, R. Al-Shdefat, S. Jamil, M. Alam, Abdel-Kader, and F. Shakeel, "Solubility of bioactive compound hesperidin in six pure solvents at (298.15 to 333.15) k," *Journal of Chemical $ Engineering Data*, vol. 59, pp. 2065–2069, 06 2014.

[79] L. Ding, X. Luo, F. Tang, J. Yuan, Q. Liu, and S. Yao, "Simultaneous determination of flavonoid and alkaloid compounds in citrus herbs by high-performance liquid chromatography–photodiode array detection–electrospray mass spectrometry," *Journal of Chromatography B*, vol. 857, no. 2, pp. 202–209, 2007.

[80] S. J. Stohs, H. G. Preuss, and M. Shara, "A review of the receptor-binding properties of p-synephrine as related to its pharmacological effects," *Oxidative Medicine and Cellular Longevity*, vol. 2011, 2011.

[81] L. G. Rossato, V. M. Costa, R. P. Limberger, M. de Lourdes Bastos, and F. Remião, "Synephrine: From trace concentrations to massive consumption in weight-loss," *Food and Chemical Toxicology*, vol. 49, no. 1, pp. 8 – 16, 2011.

[82] S. Bent, A. Padula, and J. Neuhaus, "Safety and efficacy of citrus aurantium for weight loss," *The American journal of cardiology*, vol. 94, no. 10, pp. 1359–1361, 2004.

[83] S. Haaz, K. Fontaine, G. Cutter, N. Limdi, S. Perumean-Chaney, and D. Allison, "Citrus aurantium and synephrine alkaloids in the treatment of overweight and obesity: an update," *Obesity reviews*, vol. 7, no. 1, pp. 79–88, 2006.

[84] Food, H. Drug Administration, *et al.*, "Final rule declaring dietary supplements containing ephedrine alkaloids adulterated because they present an unreasonable risk. final rule.," *Federal register*, vol. 69, no. 28, p. 6787, 2004.

[85] C.-Y. Shen, T.-X. Wang, X.-M. Zhang, and J.-G. Jiang, "Various antioxidant effects were attributed to different components in the dried blossoms of citrus aurantium l. var. amara engl," *Journal of agricultural and food chemistry*, vol. 65, no. 30, pp. 6087–6092, 2017.

[86] S. H. Lee, S. Yumnam, G. E. Hong, S. Raha, V. Venkatarame Gowda Saralamma, H. J. Lee, J. D. Heo, S. J. Lee, W.-S. Lee, E.-H. Kim, H. S. Park, and G. S. Kim, "Flavonoids of korean citrus aurantium l. induce apoptosis via intrinsic pathway in human hepatoblastoma hepg2 cells," *Phytotherapy Research*, vol. 29, no. 12, pp. 1940–1949, 2015.

[87] K.-I. Park, H.-S. Park, M.-K. Kim, G.-E. Hong, A. Nagappan, H.-J. Lee, S. Yumnam, W.-S. Lee, C.-K. Won, S.-C. Shin, *et al.*, "Flavonoids identified from korean citrus aurantium l. inhibit non-small cell lung cancer growth in vivo and in vitro," *Journal of Functional Foods*, vol. 7, pp. 287–297, 2014.

[88] A. de Moraes Pultrini, L. A. Galindo, and M. Costa, "Effects of the essential oil from citrus aurantium l. in experimental anxiety models in mice," *Life sciences*, vol. 78, no. 15, pp. 1720–1725, 2006.

[89] M. I. R. Carvalho-Freitas and M. Costa, "Anxiolytic and sedative effects of extracts and essential oil from citrus aurantium l.," *Biological and Pharmaceutical Bulletin*, vol. 25, no. 12, pp. 1629–1633, 2002.

[90] C.-Y. Shen, L. Wan, T.-X. Wang, and J.-G. Jiang, "Citrus aurantium l. var. amara engl. inhibited lipid accumulation in 3t3-l1 cells and caenorhabditis elegans and prevented obesity in high-fat diet-fed mice," *Pharmacological Research*, vol. 147, p. 104347, 2019.

[91] Ş. Karabıyıklı, H. Değirmenci, and M. Karapınar, "Inhibitory effect of sour orange (citrus aurantium) juice on salmonella typhimurium and listeria monocytogenes," *LWT-Food Science and Technology*, vol. 55, no. 2, pp. 421–425, 2014.

[92] S. Jia, Y. Hu, W. Zhang, X. Zhao, Y. Chen, C. Sun, X. Li, and K. Chen, "Hypoglycemic and hypolipidemic effects of neohesperidin derived from citrus aurantium l. in diabetic kk-a y mice," *Food & Function*, vol. 6, no. 3, pp. 878–886, 2015.

[93] M. I. El-Khaiary, "Least-squares regression of adsorption equilibrium data: comparing the options," *Journal of Hazardous Materials*, vol. 158, no. 1, pp. 73–87, 2008.

[94] Y. He, Z. Chen, H. Qu, and X. Gong, "Research progress on the separation of alkaloids from chinese medicines by column chromatography," *Advances in Chemical Engineering and Science*, vol. 10, no. 4, pp. 358–377, 2020.

[95] D. R. Kammerer, J. Kammerer, and R. Carle, "Chapter 11 - resin adsorption and ion exchange to recover and fractionate polyphenols," in *Polyphenols in Plants* (R. R. Watson, ed.), pp. 219–230, San Diego: Academic Press, 2014.

[96] S. D. Alexandratos, "Ion-exchange resins: A retrospective from industrial and engineering chemistry research," *Industrial & Engineering Chemistry Research*, vol. 48, no. 1, pp. 388–398, 2009.

[97] X. Geng, P. Ren, G. Pi, R. Shi, Z. Yuan, and C. Wang, "High selective purification of flavonoids from natural plants based on polymeric adsorbent with hydrogen-bonding interaction," *Journal of Chromatography A*, vol. 1216, no. 47, pp. 8331 – 8338, 2009. 23rd International Symposium on Microscale Bioseparations.

[98] K. Dorfner, *Ion exchangers*. Walter de Gruyter, 2011.

[99] S. D. Alexandratos, "From ion exchange resins to polymer-supported reagents: an evolution of critical variables," *Journal of Chemical Technology & Biotechnology*, vol. 93, no. 1, pp. 20–27, 2018.

[100] C. Li, Y. Ma, J. Gu, X. Zhi, H. Li, and G. Peng, "A green separation mode of synephrine from citrus aurantium l.(rutaceae) by nanofiltration technology," *Food science & nutrition*, vol. 7, no. 12, pp. 4014–4020, 2019.

[101] P. Mende and M. Wink, "Uptake of the quinolizidine alkaloid lupanine by protoplasts and isolated vacuoles of suspension-cultured lupinus polyphyllus cells. diffusion or carrier-mediated transport?," *Journal of Plant Physiology*, vol. 129, no. 3, pp. 229–242, 1987.

[102] A. Asadi Tashvigh and T.-S. Chung, "Robust polybenzimidazole (pbi) hollow fiber membranes for organic solvent nanofiltration," *Journal of Membrane Science*, vol. 572, pp. 580 – 587, 2019.

[103] E. Choe and D. Choe, "Polymeric materials encyclopedia," *CRC. Boca Raton, New York, London*, vol. 7, pp. 5379–5378, 1996.

[104] J.-T. Wang, R. Savinell, J. Wainright, M. Litt, and H. Yu, "A h2o2 fuel cell using acid doped polybenzimidazole as polymer electrolyte," *Electrochimica Acta*, vol. 41, no. 2, pp. 193–197, 1996.

[105] C. Shogbon, "B.; brousseau, jl; zhang, h.; benicewicz, bc; akpalu, y," *Macromolecules*, vol. 39, p. 9409, 2006.

[106] F. A. Ferreira, T. Esteves, M. P. Carrasco, J. Bandarra, C. A. M. Afonso, and F. C. Ferreira, "Polybenzimidazole for active pharmaceutical ingredient purification: The mometasone furoate case study," *Industrial & Engineering Chemistry Research*, vol. 58, no. 24, pp. 10524–10532, 2019.

[107] M. I. El-Khaiary, "Least-squares regression of adsorption equilibrium data: Comparing the options," *Journal of Hazardous Materials*, vol. 158, no. 1, pp. 73–87, 2008.

[108] N. Ayawei, A. N. Ebelegi, and D. Wankasi, "Modelling and interpretation of adsorption isotherms," *Journal of chemistry*, vol. 2017, 2017.

[109] T. R. Sahoo and B. Prelot, "Chapter 7 - adsorption processes for the removal of contaminants from wastewater: the perspective role of nanomaterials and nanotechnology," in *Nanomaterials for the Detection and Removal of Wastewater Pollutants* (B. Bonelli, F. S. Freyria, I. Rossetti, and R. Sethi, eds.), Micro and Nano Technologies, pp. 161–222, Elsevier, 2020.

[110] G. W. Kajjumba, S. Emik, A. Öngen, H. K. Özcan, and S. Aydın, "Modelling of adsorption kinetic processes—errors, theory and application," *Advanced sorption process applications*, pp. 187–206, 2018.

[111] S. Van Wychen and L. M. Laurens, "Determination of total carbohydrates in algal biomass: laboratory analytical procedure (lap)," tech. rep., National Renewable Energy Lab.(NREL), Golden, CO (United States), 2016.

[112] A. M. Fialho, "Protocolos das aulas laboratoriais de bioquímica e biologia molecular," *Instituto Superior Tecnico*, 2015.

[113] N. Vasconcelos, G. Pinto, and F. de ARAGAO, "Determinação de açuçares redutores pelo ácido 3, 5-dinitrosalicílico: histórico do desenvolvimento do método e estabelecimento de um protocolo para o laboratório de bioprocessos.," *Embrapa Agroindústria Tropical-Boletim de Pesquisa e Desenvolvimento (INFOTECA-E)*, 2013.

[114] H. Qiu, L. Lv, B.-c. Pan, Q.-j. Zhang, W.-m. Zhang, and Q.-x. Zhang, "Critical review in adsorption kinetic models," *Journal of Zhejiang University-Science A*, vol. 10, no. 5, pp. 716–724, 2009.

[115] F. Pellati, S. Benvenuti, and M. Melegari, "High-performance liquid chromatography methods for the analysis of adrenergic amines and flavanones in citrus aurantium l. var. amara," *Phytochemical Analysis: An International Journal of Plant Chemical and Biochemical Techniques*, vol. 15, no. 4, pp. 220–225, 2004.

Appendix A

Appendix chapter

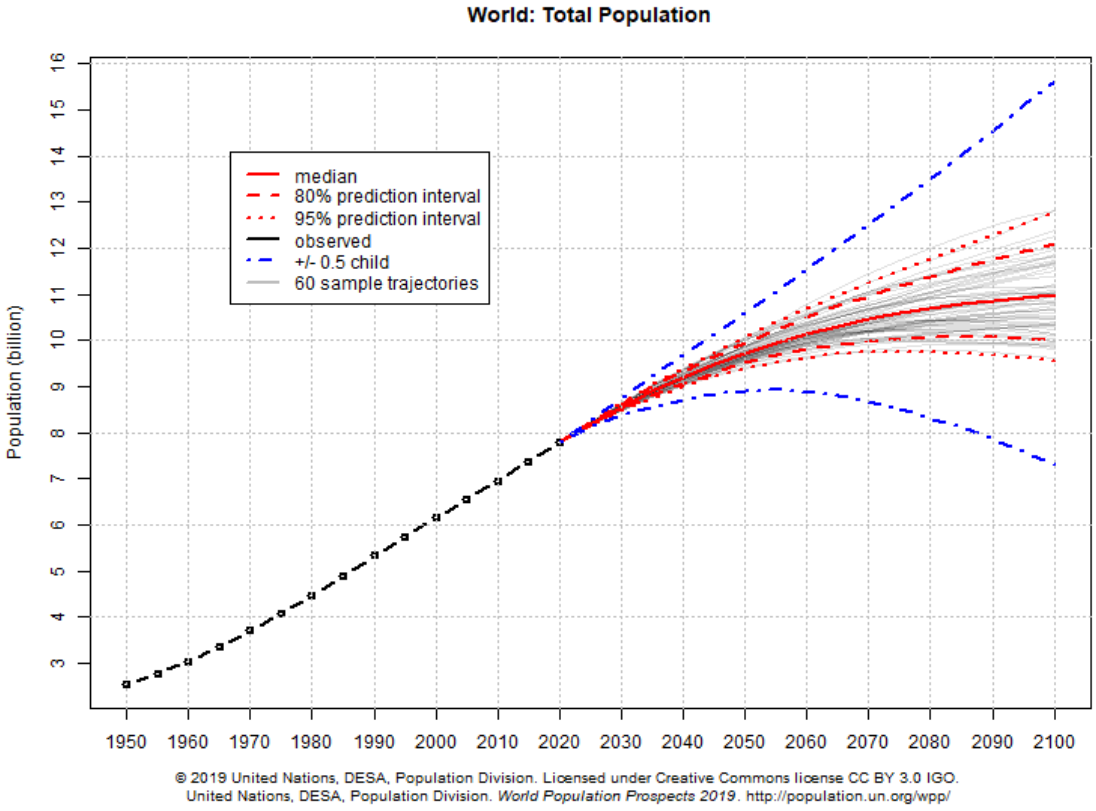

Figure A.1: Estimates and probabilistic projections of the total World population. The population projections are based on the probabilistic on the probabilistic projections of total fertility and life expectancy at birth carried out with a Bayesian Hierarchical Model (80 and 95 per cent prediction intervals of the probabilistic population projections, as well as the (deterministic) high and low variant (+/- 0.5 child).

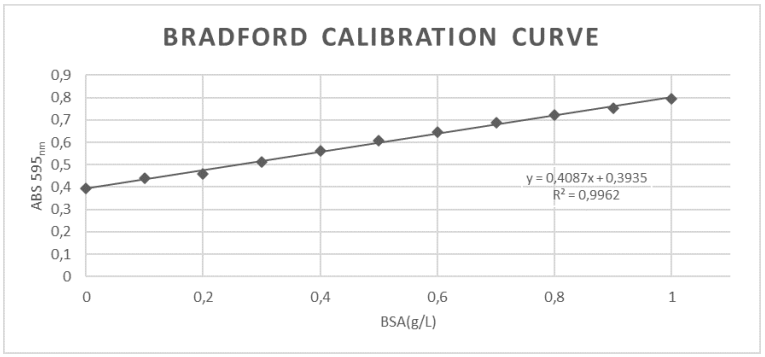

Figure A.2: Bradford Calibration curve for the different BSA Standard solutions

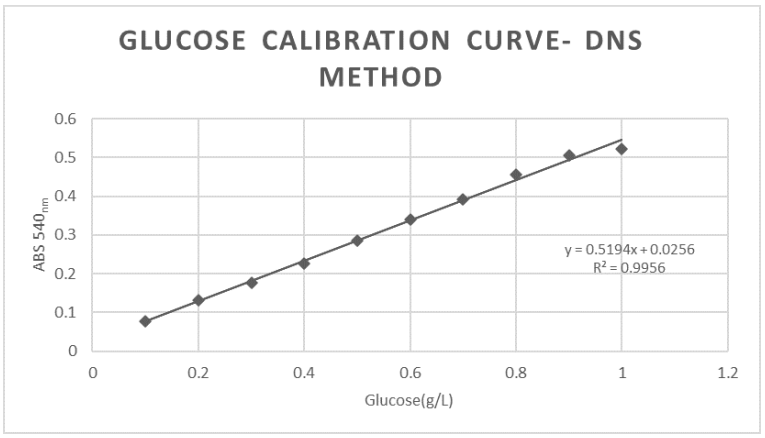

Figure A.3: DNS Calibration curve for the Glucose Standard solutions

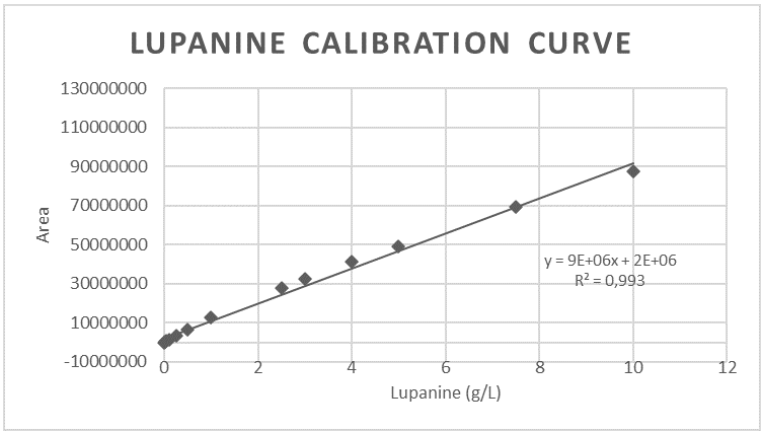

Figure A.4: Lupanine Calibration curve made from stock concentrations between 0.005 g/L and 10 g/L.

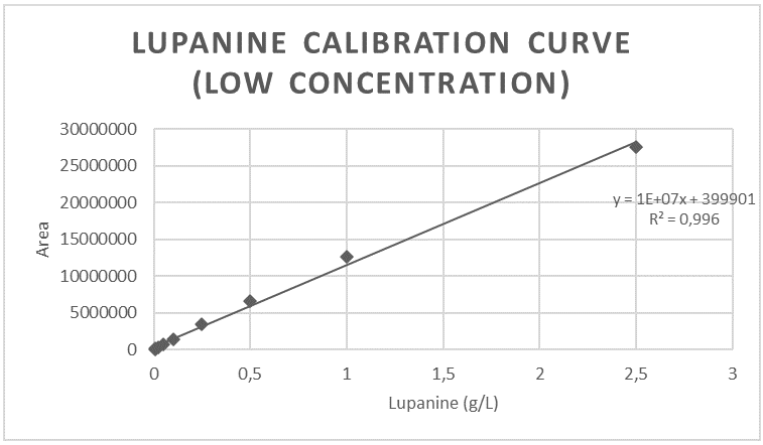

Figure A.5: New calibration curve made from the data obtained for the lower concentration of lupanine ($\leq$ 2.5 g/L) represented in Figure A.4

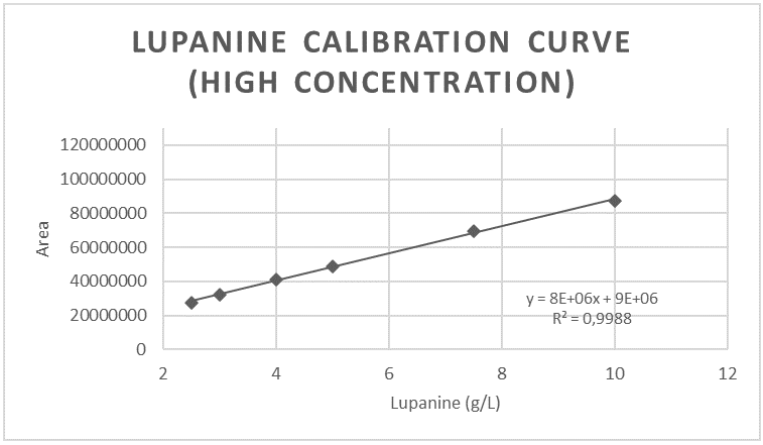

Figure A.6: New calibration curve made from the data obtained for the higher concentration of lupanine ($\geq$ 2.5 g/L) represented in Figure A.4

Figure A.7: PBI Thermal Conditioning Water Precipitation and Water Washing Step

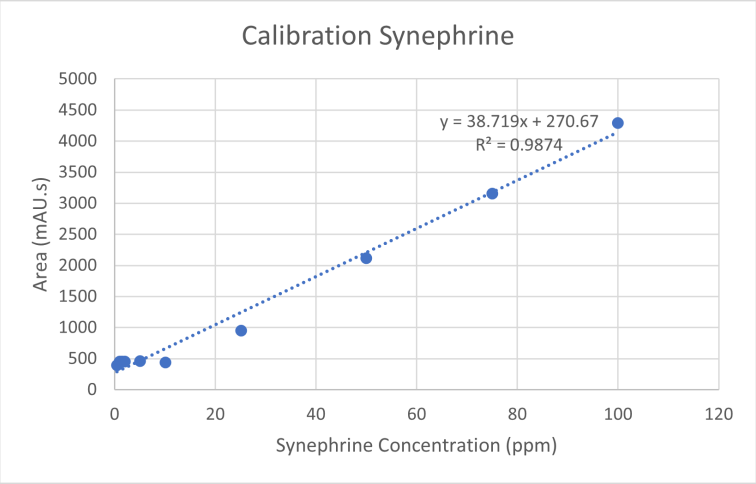

Figure A.8: Calibration curve for the synephrine Standard solutions analysed at 225nm

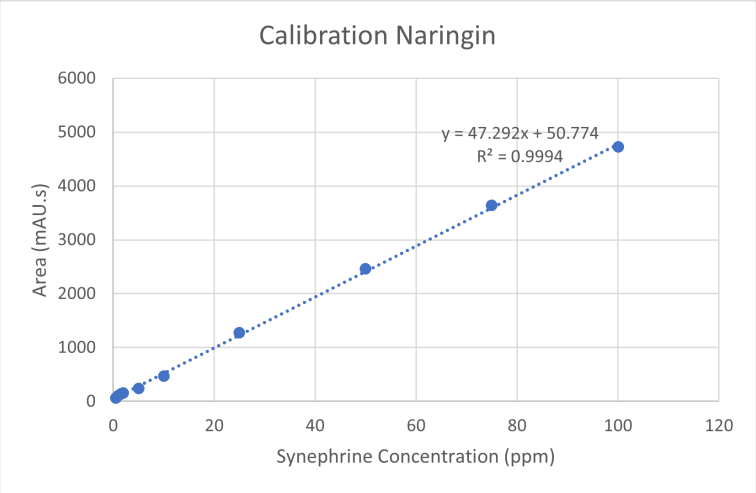

Figure A.9: Calibration curve for the naringin Standard solutions analysed at 225nm

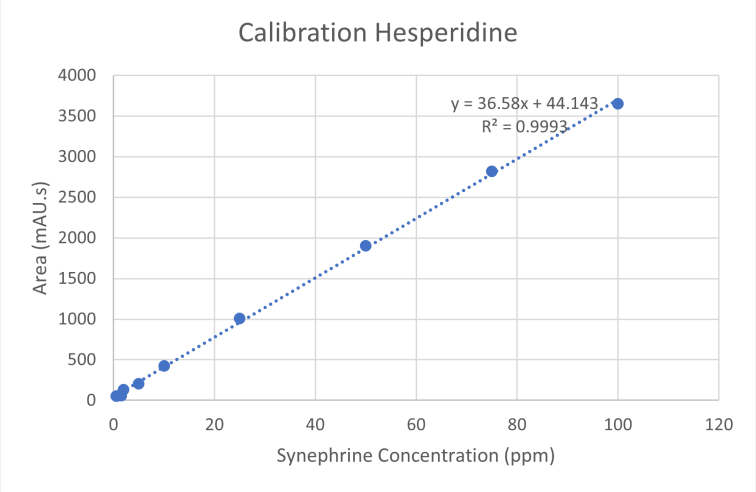

Figure A.10: Calibration curve for the Hesperidin Standard solutions analysed at 225nm

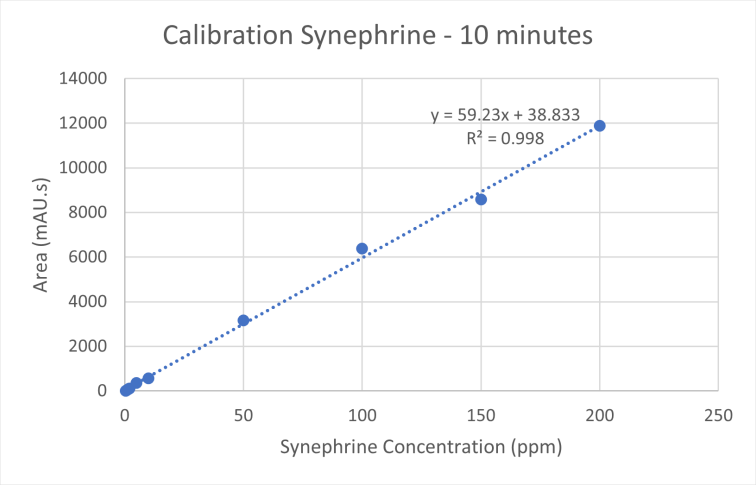

Figure A.11: Second calibration curve for the synephrine Standard solutions analysed at 225nm for pellgatiet al HPLC method

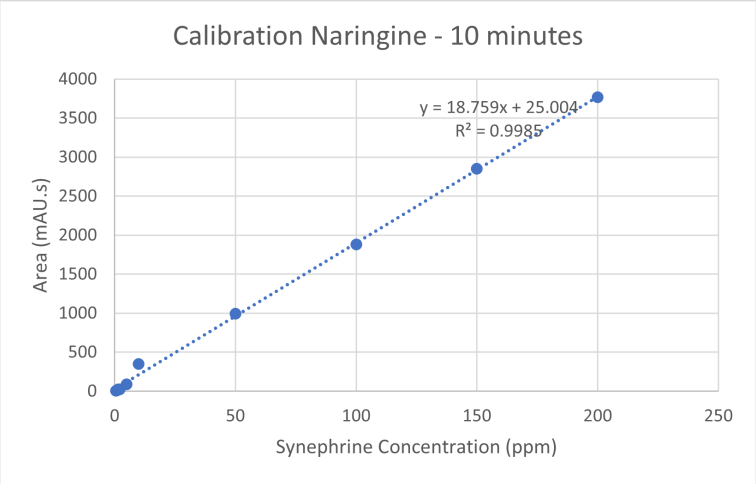

Figure A.12: Second calibration curve for the Naringin Standard solutions analysed at 283nm for pellgatiet al HPLC method

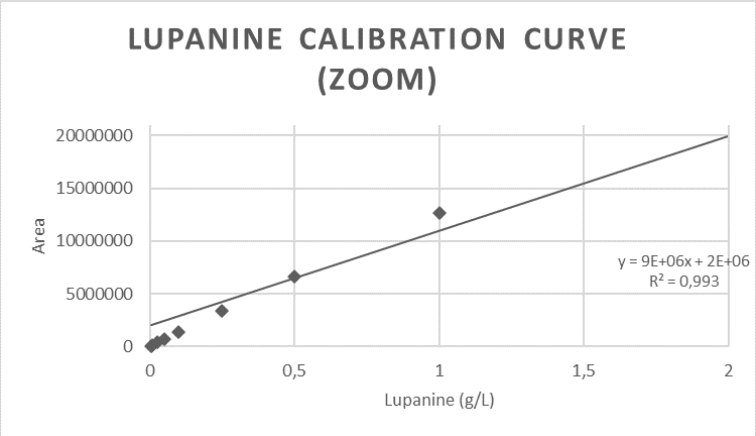

Figure A.13: - Zoom of the Lupanine Calibration curve demonstrating the lack of linearity of the calibration curve for the lower concentrations of Lupanine.

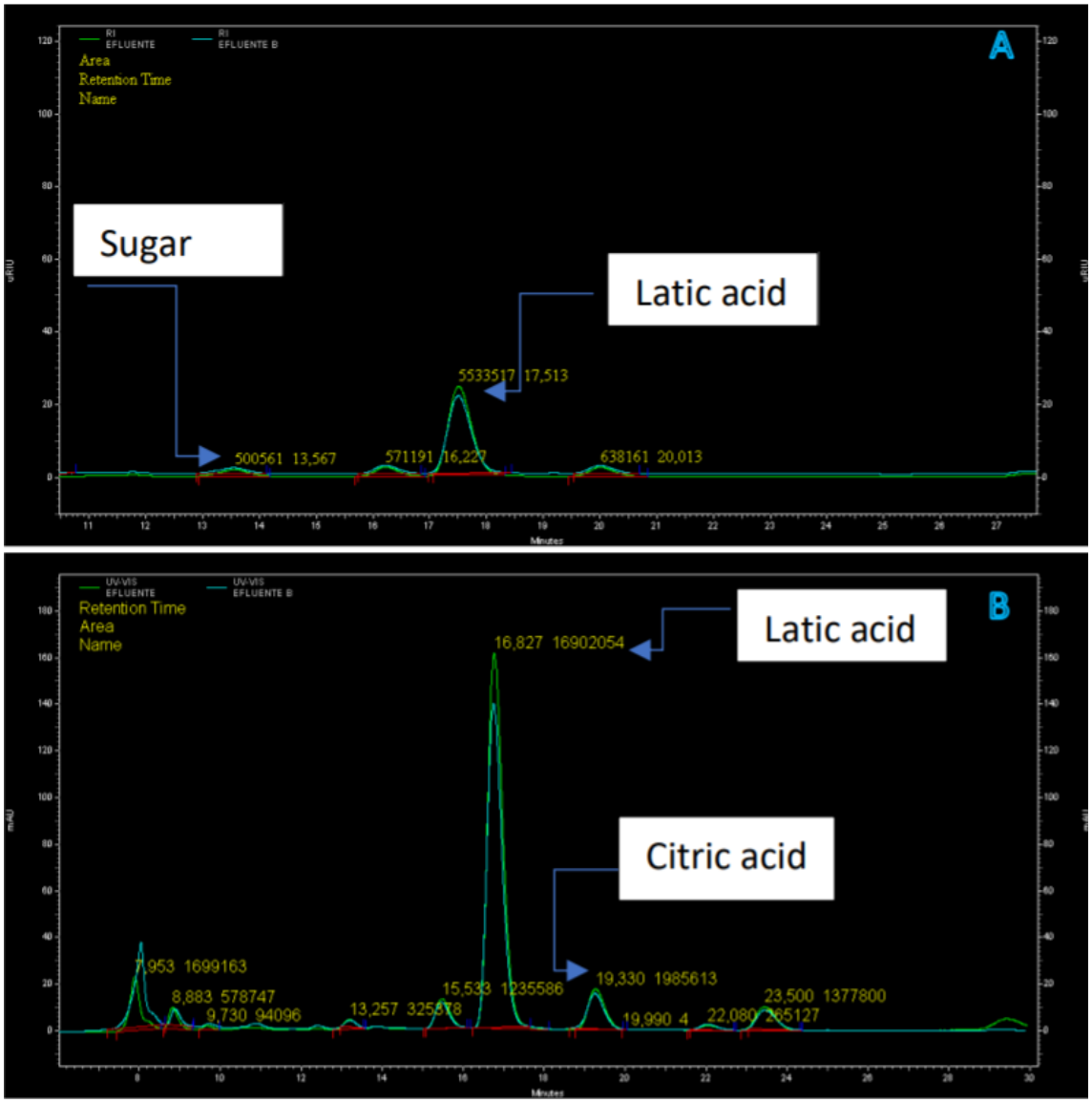

Figure A.14: RI (A) and UV-VIs (B) Chromatograms for Effluent samples at pH=5.5 (green) and pH=14 (light blue)

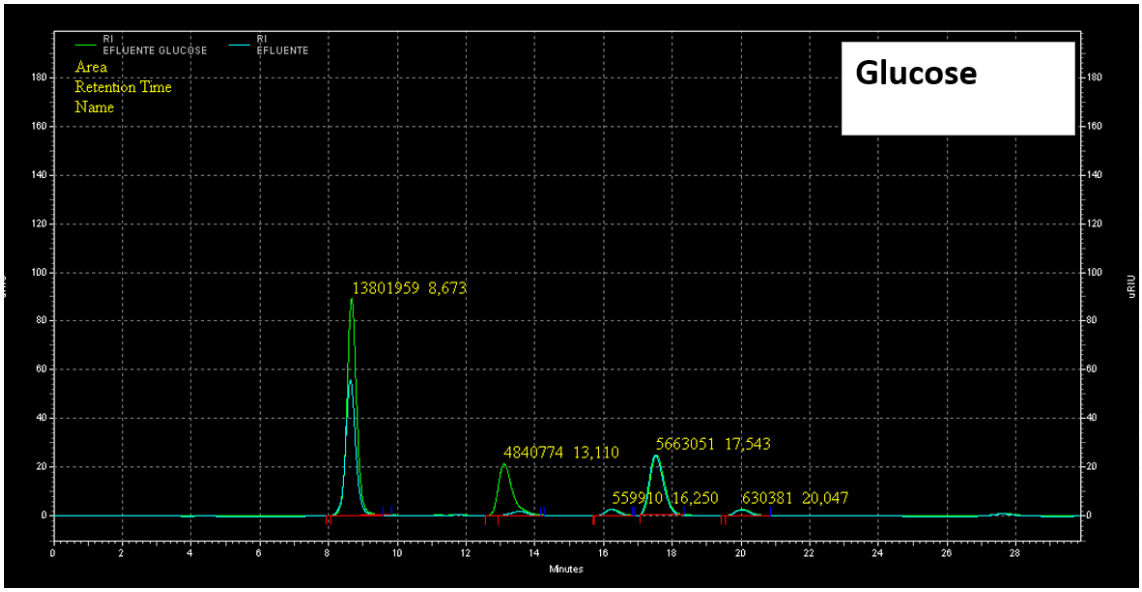

Figure A.15: RI HPLC chromatogram obtained for the effluent samples at pH=5.5 with glucose internal standard (green) and without (light blue)

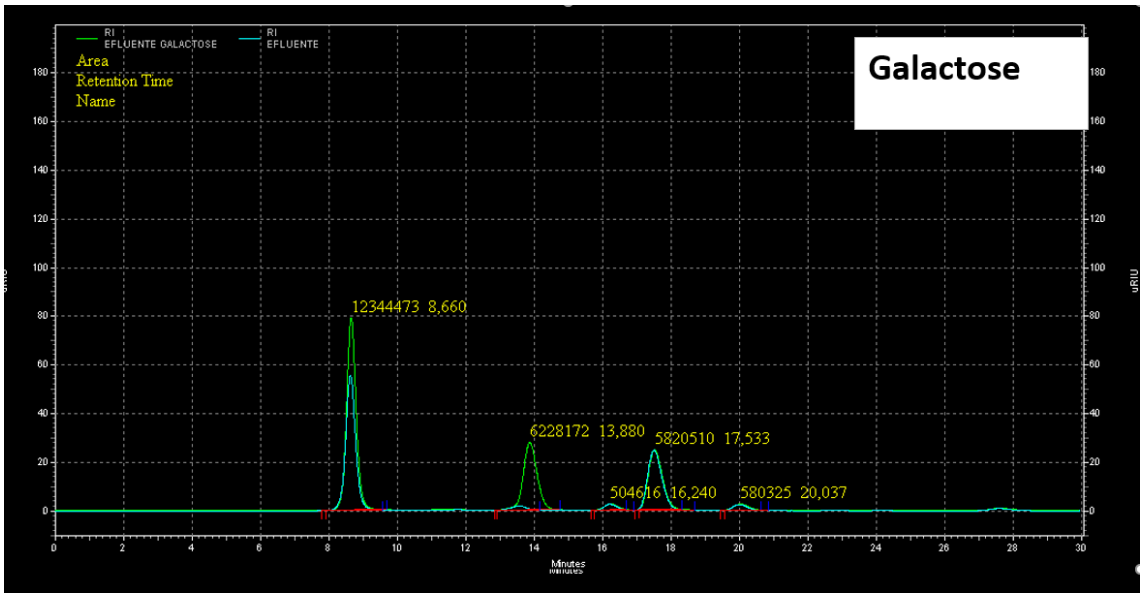

Figure A.16: RI HPLC chromatogram obtained for the effluent samples at pH=5.5 with galactose internal standard (green) and without (light blue)

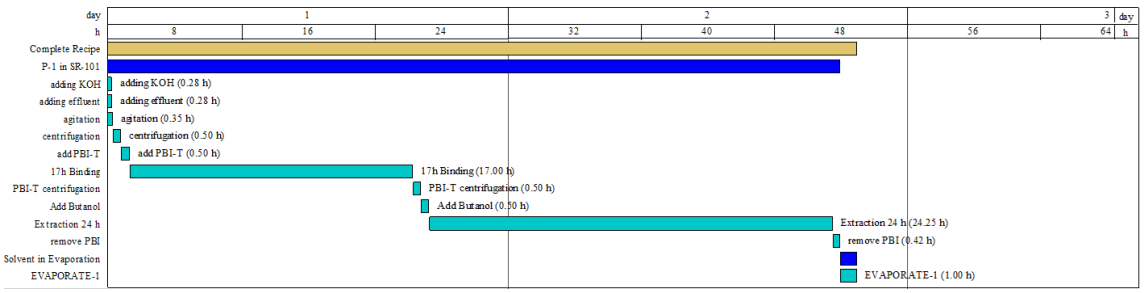

Figure A.17: Lupanine Industrial Gantt Chart for the Case Study 1 and 2

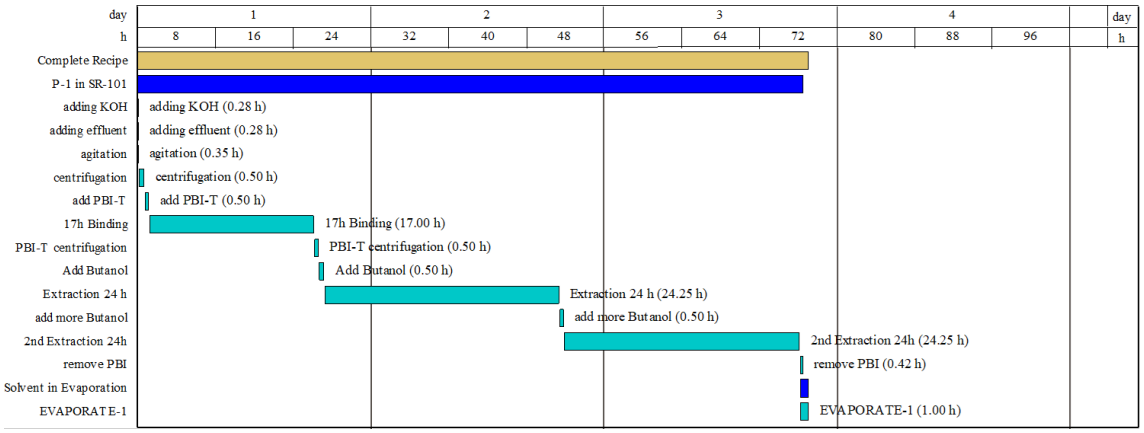

Figure A.18: Lupanine Industrial Gantt Chart for the Case Study 3

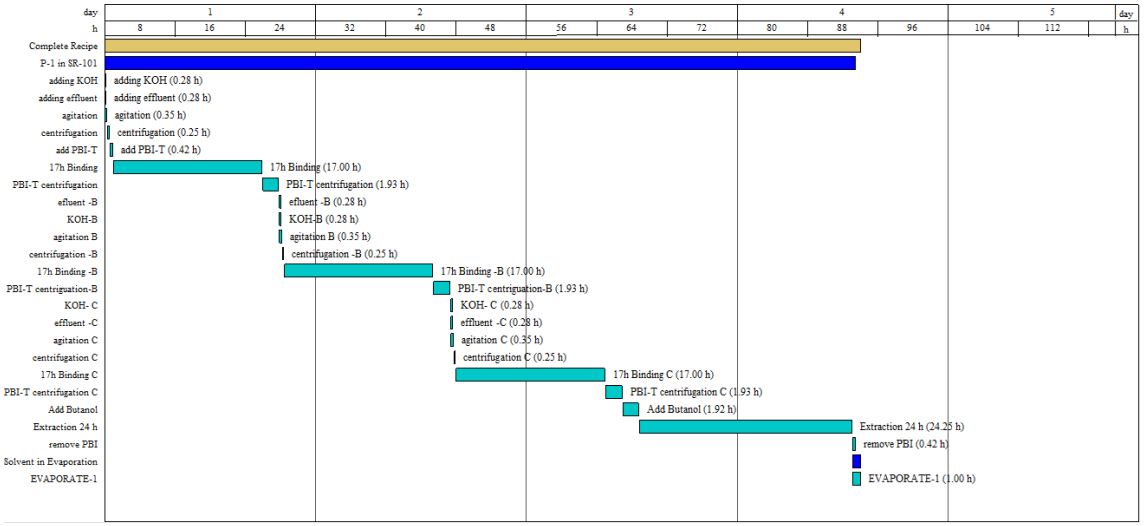

Figure A.19: Lupanine Industrial Gantt Chart for the Case Study 4

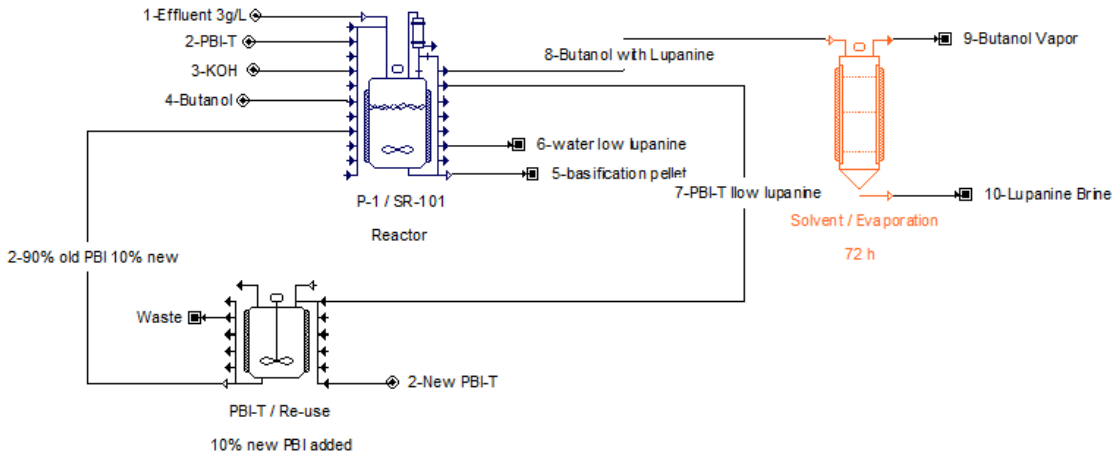

Figure A.20: Example of Flow Sheet to recirculate PBI-T on Lupanine Industrial process

Economic Evaluation Report
for Case Study 4

1. EXECUTIVE SUMMARY For Case Study 4 (2021 prices)

Total Capital Investment	5,636,000 $
Capital Investment Charged to This Project	827,000 $
Operating Cost	8,247,000 $/yr
Revenues	10,819,000 $/yr
Batch Size	5.88 kg MP
Cost Basis Annual Rate	540.93 kg MP/yr
Unit Production Cost	15,246.13 $/kg MP
Net Unit Production Cost	15,246.13 $/kg MP
Unit Production Revenue	20,000.00 $/kg MP
Gross Margin	23.77 %
Return On Investment	186.67 %
Payback Time	0.54 years
IRR (After Taxes)	36.95 %
NPV (at 7.0% Interest)	7,515,000 $

MP = Flow of Component 'lupanine' in Stream 'Lupanine Brine'

2. MAJOR EQUIPMENT SPECIFICATION AND FOB COST (2021 prices)

Quantity/ Standby/ Staggered	Name	Description	Unit Cost ($)	Cost ($)
1 / 0 / 0	SR-101	Stirred Reactor Vessel Volume = 1238.80 L	609,000	609,000
1 / 0 / 0	Evaporation	Thin Film Evaporator Film Area = 2.09 m2	155,000	155,000
				764,000
			TOTAL	

3. LABOR COST - PROCESS SUMMARY

Labor Type	Unit Cost ($/h)	Annual Amount (h)	Annual Cost ($)	%
Operator	69.00	11,585	799,371	100.00
TOTAL		11,585	799,371	100.00

4. MATERIALS COST - PROCESS SUMMARY

Bulk Material	Unit Cost ($)	Annual Amount		Annual Cost ($)	%
Butanol	955.35	74	MT	70,815	2.63
efluent 3g/L	0.00	274,543	kg	0	0.00
KOH	0.35	5,106	kg	1,779	0.07
PBI-T	284.53	9,200	kg	2,617,676	97.30
TOTAL				2,690,269	100.00

5. UTILITIES COST (2021 prices) - PROCESS SUMMARY

Utility	Unit Cost ($)	Annual Amount	Ref. Units	Annual Cost ($)	%
Std Power	0.10	665	kW-h	66	14.06
Evaporator Steam	12.00	34	MT	406	85.94
TOTAL				473	100.00

6. ANNUAL OPERATING COST (2021 prices) - PROCESS SUMMARY

Cost Item	$	%
Raw Materials	2.690.000	32.62
Labor-Dependent	799.000	9.69
Facility-Dependent	4.717.000	57.20
Laboratory/QC/QA	40.000	0.48
TOTAL	8.247.000	100.00

7. PROFITABILITY ANALYSIS (2021 prices)

A.	Direct Fixed Capital	5,063,000 $
B.	Working Capital	320,000 $
C.	Startup Cost	253,000 $
D.	Up-Front R&D	0 $
E.	Up-Front Royalties	0 $
F.	Total Investment (A+B+C+D+E)	5,636,000 $
G.	Investment Charged to This Project	827,000 $
H.	Revenue/Savings Rates	
	Lupanine Brine (Main Revenue)	541 kg /yr
I.	Revenue/Savings Price	
	Lupanine Brine (Main Revenue)	20,000.00 $/kg
J.	Revenues/Savings	
	Lupanine Brine (Main Revenue)	10,818,699 $/yr
1	Total Revenues	10,818,699 $/yr
2	Total Savings	0 $/yr
K.	Annual Operating Cost (AOC)	
1	Actual AOC	8,247,000 $/yr
2	Net AOC (K1-J2)	8,247,000 $/yr
L.	Unit Production Cost /Revenue	
	Unit Production Cost	15,246.13 $/kg MP
	Net Unit Production Cost	15,246.13 $/kg MP
	Unit Production Revenue	20,000.00 $/kg MP
M.	Gross Profit (J-K)	2,572,000 $/yr
N.	Taxes (40%)	1,029,000 $/yr
O.	Net Profit (M-N + Depreciation)	1,543,000 $/yr
	Gross Margin	23.77 %
	Return On Investment	186.67 %
	Payback Time	0.54 years

MP = Flow of Component 'lupanine' in Stream 'Lupanine Brine'

Figure A.21: Economic Evaluation Report for Case Study 4 obtained in Superpro Designer v10.3

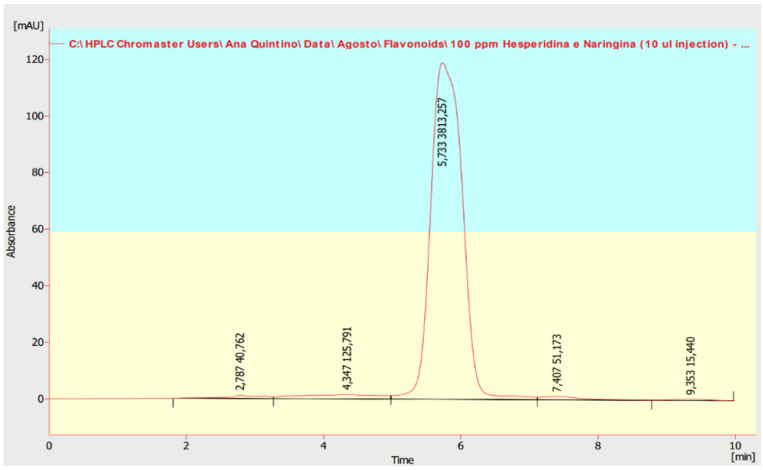

Figure A.22: First HPLC chromatogram obtained for Hesperidin and Naringin using HPLC method from [114]

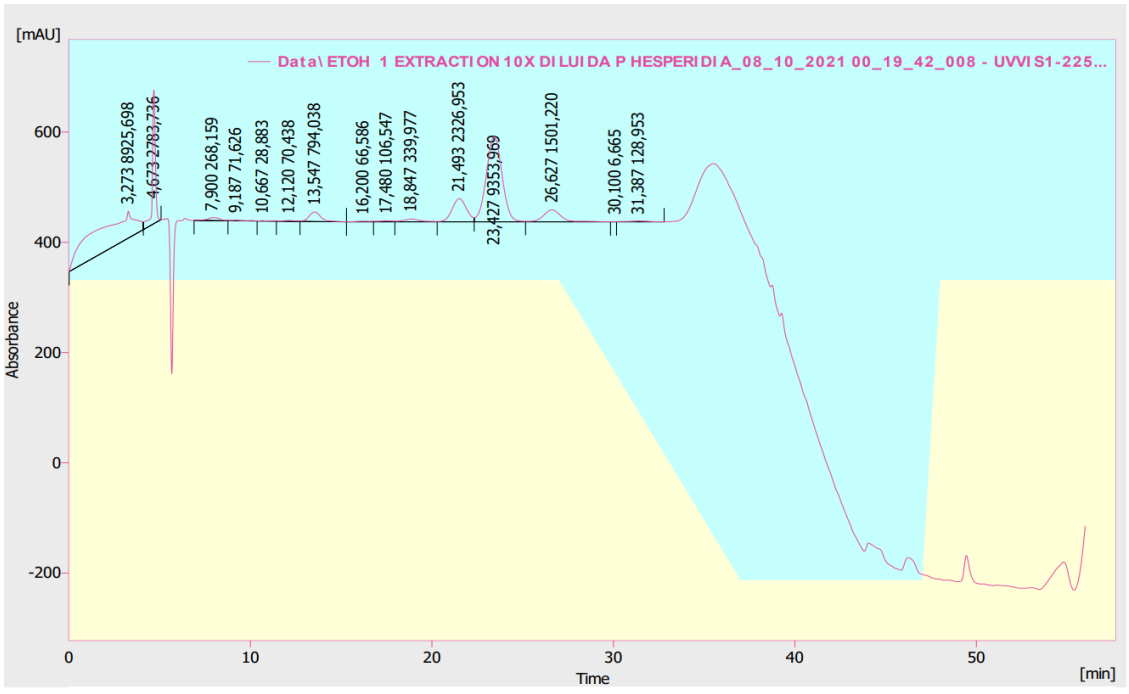

Figure A.23: HPLC chromatogram obtained for the ethanol Extraction with Hesperidin as internal standard